J. CHEM. SOC. FARADAY TRANS., 1995, 91(21), 3755–3770

UV-induced Isomerization of (*E*)-Crotonic Acid

Combined Matrix-isolated IR and *ab initio* MO Study

Rui Fausto*
Departamento de Química, Universidade de Coimbra, P-3049 Coimbra, Portugal
Anatoly Kulbida
Institute of Physics, St. Petersburg University, Peterhof, 198904 St. Petersburg, Russia
Otto Schrems
Alfred-Wegener Institut fur Polar und Meeresforschung, Postfach 120161, D-27515 Bremerhaven, Germany

The results of a combined vibrational and structural study of the (*E*)-crotonic acid monomer undertaken by matrix-isolated low-temperature IR spectroscopy and *ab initio* SCF-MO calculations are presented. It is shown that in both argon and krypton matrices monomeric (*E*)-crotonic acid exists as a mixture of two conformers of similar energies, differing by the relative orientation of the C=C—C=O axis (the s-*cis* and s-*trans* forms, having a C=C—C=O dihedral angle equal to 0° and 180°, respectively). Upon UV-irradiation in the 240–250 nm region by a xenon lamp, photoisomerization reactions about both C_α—C and C=C bonds occur leading, respectively, to s-*cis* → s-*trans* (*E*)-crotonic acid rotamerization and (*E*)-crotonic acid → (*Z*)-crotonic acid conversion. Results of *ab initio* SCF-MO calculations, in particular optimized geometries, relative stabilities, dipole moments and harmonic force fields, for the relevant conformational states of both (*E*) and (*Z*)-crotonic acids are also presented and the conformational dependence of some relevant structural parameters is used to characterize the most important intramolecular interactions present in the studied forms. Finally, results of a normal mode analysis based on the *ab initio* calculated vibrational spectra are used to help interpret the experimenal vibrational data, enabling a detailed assignment of the matrix-isolated spectra and the characterization of the observed photoinduced isomerization reactions.

α,β-Unsaturated carbonylic-based materials (polymers) have a wide range of practical commercial applications and have been widely studied.[1–3] However, despite the relevance of these systems, their precursors (monomers) have neither been systematically studied in detail nor characterized well, either structurally or spectroscopically. On the other hand, α,β-unsaturated carbonylic molecules have also been proven to be of fundamental importance to the study of some catalytic reactions involving serine proteases (*e.g.* chymotrypsin),[4–6] since they can be successfully used as *in situ* resonance Raman spectroscopic probes of the enzyme–substrate transient complexes formed within the enzyme's active site during catalysis.[4,5] Indeed, in this field of research, a detailed knowledge of conformational preferences and vibrational properties of simple molecules containing the C=C—C=O fragment assumes particular relevance, as stressed elsewhere.[4,5]

It has been recently shown that these kinds of molecules undergo UV-induced isomerization reactions about either C_α—C or C=C bonds.[7–10] In a previous study, we have studied the first of these two types of isomerization reactions in monomeric acrylic acid isolated in noble-gas matrices at low temperatures and we have observed that irradiation at $\lambda = 243$ nm promotes s-*cis* → s-*trans* rotamerization.[9] On the other hand, photoinduced isomerization reactions about the C=C bond in β-substituted α,β-unsaturated carboxylic molecules of general formula R=CH=CH—C(=O)OR′ (R, R′ = H or alkyl), leading to *cis* → *trans* isomerization about this bond, have also been observed to occur when, for instance, these molecules are exposed to UV-laser beam of appropriate wavelength[10–12] (a very interesting example of this kind of photochemical reaction was reported some years ago, in a study of the *trans* → *cis* isomerization about the C=C bond that takes place during the recording of resonance Raman spectra of α,β-unsaturated carboxylic esters bound to serine proteases.[10]) In addition to their relevance to the biochemical studies on serine proteases, these types of photochemical reactions appears also to be potentially useful in organic synthesis, thus stressing the interest of looking at them in greater detail.

To the best of our knowledge, no studies on the molecular structure and vibrational properties of either (*E*)- or (*Z*)-crotonic acid monomers have been reported until now, despite a series of publications that have reported on their dimers.[13–15] At least in part, this is due to the practical difficulty of handling the monomeric structures, which strongly tend to polymerize under current experimental conditions.[16] Since matrix isolation spectroscopy provides a unique way of studying these species, this technique was used in the present study to obtain the IR spectrum of (*E*)-crotonic acid and to study the rotamerization processes taking place upon sample irradiation by UV light. To aid interpretation of the experimental data, a series of *ab initio* molecular orbital calculations have been performed using the 6-31G* basis set, which includes one set of polarization functions in all non-hydrogen atoms (it is well known that, for systems containing conjugated double bonds, reliable structural and vibrational results can, in general, only be achieved if at least polarization functions on all non-hydrogen atoms are included in the basis set[17,18]). Besides the molecular structures and relative energies of the various stable conformations of both (*Z*)- and (*E*)-crotonic acids, theoretical calculations of the vibrational spectra of the individual conformers, complemented by normal mode calculations based on the 6-31G* theoretical harmonic force fields, have also been carried out, providing us with very valuable information for the assignment of the experimental spectra.

Experimental and Computational Methods

(*E*)-crotonic acid (>99% purity) was obtained from Aldrich and purified by several freeze–pump–thaw cycles. Ar and Kr were obtained from Messer Griesheim GmbH and were,

respectively, of 99.999% and 99.998% purity. All matrices were prepared in a conventional way by deposition of the gaseous mixture on a gold-plated copper mirror, cooled using a ROK 10-300 (Leybold-Heraeus) closed-cycle refrigerator. The deposition temperatures, measured at the mirror with a silicon diode and a DRC 93C temperature controller (Lake Shore Cryotonics), were 14 or 18 K (Ar) and 25 K (Kr). The matrix: solute ratios were *ca.* 1500 and the rates of the matrix gas flow *ca.* 5.0×10^{-3} (Ar) or 1.5×10^{-3} mol h^{-1} (Kr). Further details on the sample preparation procedure can be found in ref. 19.

The IR spectra were recorded in reflection mode (0.5 cm^{-1} resolution) on a Bruker IFS 66V Fourier transform spectrometer equipped with a germanium/CsI beam splitter and with a DTGS detector fitted with CsI windows. The irradiation of the samples was carried out using a UV light source (L.O.T.-Oriel GmbH) whose main component is a 500 W Xe arc lamp. The collimated UV beam irradiated the sample through the Suprasil window of the cryostat after being filtered through both a water filter and an interference filter of the FS10-50 type with a bandwidth of *ca.* 8–10 nm (L.O.T.-Oriel GmbH).

The *ab initio* SCF-MO calculations were carried out using the 6-31G* basis set[20] and the GAUSSIAN 92 program[21] on a DEC ALPHA 7000 computer. Molecular geometries were fully optimized by the force gradient method using Berny's algorithm.[22] The largest residual coordinate forces were always $< 3 \times 10^{-4}\ E_h\ a_0^{-1}$ (or E_h rad^{-1})† for bond stretches and angle bends, respectively. The force constants (symmetry internal coordinates) to be used in the normal coordinate analysis were obtained from the *ab initio* Cartesian harmonic force constants using the program TRANSFORMER.[23] This program was also used to prepare the input data for the normal coordinate analysis programs used in this study (BUILD-G and VIBRAT[24]). The calculated force fields were then scaled down by using a simple linear regression for each symmetry class in order to adjust the calculated frequencies to the experimental frequencies (two scale factors were obtained: one related to the in-plane vibrations, and the other to the out-of-plane modes). Non-observed bands (or bands doubtfully ascribable using only a pure empirical approach) were then calculated from the corresponding force fields by interpolation using the straight lines obtained previously. While very simple, this scaling procedure preserves the potential-energy distributions (PEDs) as they emerge from the *ab initio* calculations, thus having an important advantage over the more elaborate force-field scaling procedures that use more than one scale factor for each symmetry class that usually give rise to important PEDs distortions from the *ab initio* calculated values.

Results and Discussion

Molecular Orbital Calculations (Geometries and Energies)

In general, α,β-unsaturated carboxylic compounds exist as a mixture of s-*cis* and s-*trans* conformers about the C_α—C bond (Fig. 1), with the s-*cis* form corresponding to the conformational ground state.[9,14–16,25,26] The main factors that are responsible for the relative energy of these two forms are now well understood:[9,14,25] (i) mesomerism within the carboxylate group (canonical form **II** in Fig. 2), (ii) mesomerism involving both C=C and C=O double bonds (canonical form **III** in Fig. 2) and (iii) steric repulsions between the CRH=CH (R = alkyl) moiety and the oxygen atoms. The first factor is the most important one and, together with the third, favours the s-*cis* conformer; the second factor favours the s-*trans* conformer. On the whole, these interactions make the s-*cis* form slightly more stable than the s-*trans* conformer.

A second degree of conformational freedom in the studied molecules is related to the internal rotation about the C—O single bond (see Fig. 1). In general, carboxylic acids adopt the s-*cis* conformation about this bond (O=C—O—H dihedral angle = 0°), both the energy difference between this conformation and the second stable conformation (most of the time the planar s-*trans* conformation corresponds to an O=C—O—H dihedral angle = 180° but, sometimes when strong steric repulsions are present, to a non-planar structure with an O=C—O—H angle in the 150–170° region[27,28]) and the energy barrier for interconversion between these two forms being usually very large (over 20 and 40 kJ mol^{-1}, respectively[9,27–30]). The main factor that determines the much lower energy of the s-*cis* O=C—O—H axis when compared with that of the s-*trans* O=C—O—H axis is the presence in the latter of the strongly stabilizing through-space field interaction resulting from the nearly antiparallel align-

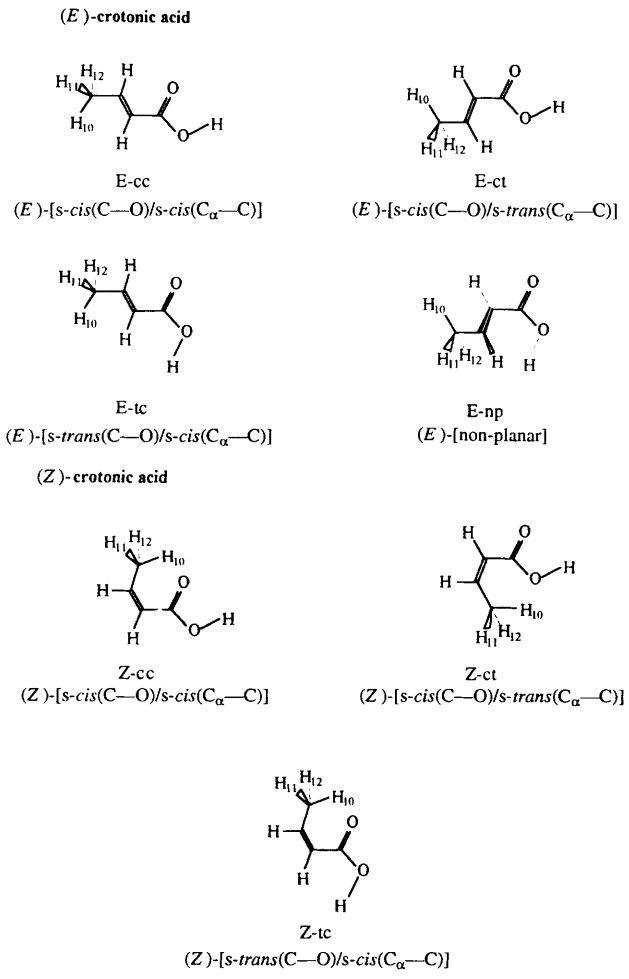

Fig. 1 Conformers of (*E*)- and (*Z*)-crotonic acid (monomer) and atom numbering

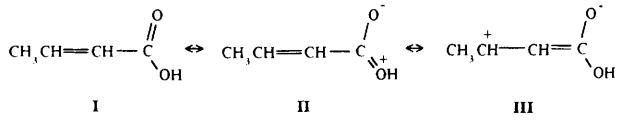

Fig. 2 Canonical forms of crotonic acids showing (**II**) mesomerism within the carboxylate group and (**III**) mesomerism associated with the two double bonds

† 1 E_h = 2625.5001 kJ mol^{-1}; 1 a_0 = 5.291 77 × 10^{-11} m.

ment of the C=O and O—H bond dipoles.[29] In general, the higher energy conformers are not observed spectroscopically under the present experimental conditions, unless particular specific intramolecular stabilizing interactions are operating (as, for instance, intramolecular hydrogen bonding in chloroacetic acid monomer[19,31]).

(*E*)-*Crotonic Acid*

Table 1 shows the calculated molecular geometries, rotational constants and energies for the various possible conformers of (*E*)-crotonic acid. As expected, the s-*cis*(C—O) conformers (E-cc and E-ct; see Fig. 1) have a considerably lower energy than the s-*trans*(C—O) and non-planar forms (E-tc and E-np; see Fig. 1). The conformational ground state corresponds to the E-cc form, where both O=C—O—H and C=C—C=O dihedral angles are equal to 0°. The second s-*cis*(C—O) form (E-ct, which has the C=C—C=O axis assuming the *s-trans* conformation) has a slightly higher energy than this form ($\Delta E_{(\text{E-ct})-(\text{E-cc})} \approx 2.8$ kJ mol^{-1}), while E-tc and E-np have energies *ca.* 30.0 and 38.0 kJ mol^{-1} above that of the most stable form.

The calculated energy difference between the two s-*cis*(C—O) forms is similar to that previously obtained for methyl (*E*)-crotonate using a 4-31G basis set (2.99 kJ mol^{-1} [14]) and comparable to the enthalpy difference obtained for the latter molecule in the pure liquid phase from temperature-variation IR spectroscopic studies (2.65 ± 0.27 kJ mol^{-1} [14]). Taking into consideration the comparable *ab initio* values, then the slightly lower $\Delta E_{(\text{E-ct})-(\text{E-cc})}$ value found for (*E*)-crotonic acid when compared with that obtained for methyl (*E*)-crotonate can be explained considering that the s-*cis* stabilization due to the mesomerism within the

Table 1 6-31G* calculated optimized geometries, rotational constants, energies and electric dipole moments for the various conformers of (*E*)- and (*Z*)-crotonic acids

	(*E*)-crotonic acid				(*Z*)-crotonic acid		
	s-*cis*(C—O)		s-*trans*(C—O)		s-*cis*(C—O)		s-*trans*(C—O)
	s-*cis*	s-*trans*	s-*cis*		s-*cis*	s-*trans*	s-*cis*
parameter	E-cc	E-ct	E-tc	E-np	E-cc	E-ct	E-tc
				bond length/pm			
C=O	119.15	119.05	118.50	118.34	119.20	119.07	118.54
C—O	133.13	133.37	133.59	133.60	133.27	133.22	133.72
C_α—C	147.83	147.68	148.75	149.03	147.96	148.00	148.82
C=C	132.28	132.29	132.27	132.23	132.67	132.66	132.73
C—C	149.76	149.86	149.73	150.00	149.98	150.06	149.93
C_α—H	107.44	107.45	107.79	107.48	107.39	107.40	107.75
C_β—H	107.68	107.61	107.65	107.96	107.86	107.87	107.87
C—H(10)	108.33	113.88	108.34	108.29	107.66	107.63	107.61
C—H(11)	108.64	118.90	108.62	108.60	108.71	108.69	108.70
C—H(12)	108.64	118.90	108.62	108.62	108.71	108.69	108.70
O—H	95.20	95.18	94.71	94.66	95.19	95.23	94.69
				bond angle/degrees			
O=C—O	122.08	121.90	120.16	120.49	121.51	121.37	119.52
C—C=O	126.07	123.79	124.31	121.97	127.72	122.45	125.89
C—C—O	111.85	114.31	115.53	117.54	110.77	116.18	114.59
H—C_α—C	116.93	113.88	118.64	113.47	114.64	111.26	116.34
C=C_α—C	120.53	124.01	120.53	125.22	125.77	129.80	125.95
H—C_β=C	117.89	118.90	117.58	119.96	115.85	115.05	115.79
C—C_β=C	125.10	124.62	125.30	124.84	129.58	131.25	129.67
C—O—H	107.88	107.55	112.22	111.83	107.79	107.19	112.42
H(10)—C—C	111.87	111.82	112.02	111.54	112.73	113.47	112.72
H(11)—C—C	110.35	110.38	110.27	110.43	109.31	109.21	109.18
H(12)—C—C	110.35	110.38	110.27	110.55	109.31	109.21	109.18
C—C(=O)—O	180.00	180.00	180.00	180.36	180.00	180.00	180.00
H—C—C=O	180.00	0.00	180.00	−20.45	180.00	0.00	180.00
C=C—C=O	0.00	180.00	0.00	154.93	0.00	180.00	0.00
H—C=C—C	0.00	0.00	0.00	1.48	180.00	180.00	180.00
C—C=C—C	180.00	180.00	180.00	183.30	0.00	0.00	0.00
O=C—O—H	0.00	0.00	180.00	168.17	0.00	0.00	180.00
H(10)—C—C=C	0.00	0.00	0.00	−1.56	0.00	0.00	0.00
H(11)—C—C=C	121.74	120.94	121.04	119.17	121.74	121.82	121.81
H(12)—C—C=C	−121.74	−120.94	−121.04	−122.41	−121.74	−121.82	−121.81
				rotational constant/MHz			
A	11376.27	10140.44	10118.28	9728.16	8228.26	7934.23	8191.66
B	1917.28	1950.79	1926.86	1942.50	2440.67	2486.77	2438.09
C	1634.36	1652.51	1624.71	1650.71	1904.09	1915.35	1900.56
				conformer energy/kJ mol^{-1}			
ΔE^a	—	2.838	30.501	38.318	10.529	17.605	41.093
	—	(2.736)	(29.313)	(37.414)	(11.054)	(18.107)	(40.262)
				dipole moment/D[b]			
$\lvert\mu\rvert$	1.957	2.899	5.102	5.598	1.580	2.810	4.702

[a] Energies relative to the most stable conformer; values presented in parentheses are relative energies including zero-point vibrational energy corrections. The total energy for the most stable form is, −304.696 34 17 (E_h). [b] 1 D = 3.335 64 × 10^{-30} C m.

C(=O)OX (X=H, CH_3) fragment is more important in the ester than in the acid, owing to the additional electron charge release from the methyl group towards the ester oxygen atom. On the other hand, the higher value now obtained for this energy difference when compared with that calculated using the same basis set (6-31G*) for monomeric acrylic acid (1.8 kJ mol^{-1} [9]) can be correlated with the different relative orientation and magnitude of the bond dipoles of the two conformers in (*E*)-crotonic and acrylic acids (Fig. 3), the decisive factor being the opposite direction of polarization of the C=C bond in these two molecules. Indeed, a similar result has been previously obtained for the methyl esters of acrylic and (*E*)-crotonic acids.[14]

It is important to note that the geometrical changes observed upon E-cc → E-ct conformational interconversion (see Table 1) are consistent with the relative importance in these two forms of the three factors referred to above which determine their relative energy. Thus, an increased importance of the mesomerism within the carboxylate group (**II** in Fig. 2) in the E-cc form makes the C—O bond shorter in this form, while a prevalence of the mesomerism involving both C=C and C=O double bonds (**III** in Fig. 2) in the E-ct conformer leads to a shorter C_α—C bond is this form. Note, the C=O bond length is larger in the most stable E-cc form, indicating that the conjugated effect of the two stabilizing mesomeric effects (both contributing to increase this bond length) is globally more important in this form. In turn, the greater importance of the destabilizing steric repulsions between the CRH=CH (R = alkyl) moiety and the —O— atom in the E-ct form, when compared with the CRH=CH/O= repulsions in the E-cc form, reflects clearly in the relative values of the C—C=O, C—C—O, H—C_α—C, C=C_α—C and H—C_β=C angles in the two conformers. Thus, the C—C=O and H—C_α—C angles reduce in going from the E-cc to the E-ct conformer, while the remaining angles increase. More important steric interactions between α-substituents and the —O— atom, compared with repulsions involving the carbonyl oxygen, have been previously found in other α-substituted carbonyl compounds, including acrylic acid,[9,25–29] and this seems to be a general trend that usually has important geometrical implications.

The planar high energy E-tc conformer has an energy relative to the most stable conformer that is almost equal to the energy difference between the equivalent conformers in acrylic acid (30.0 kJ mol^{-1} [9]). This clearly shows that the β-substitution of H by CH_3 is not relevant in determining this quantity. Thus, this result is in consonance with our previous conclusion that the relative energy of s-*cis* (C—O) and s-*trans*(C—O) forms are essentially determined by the through-space field interaction between the C=O and O—H bond

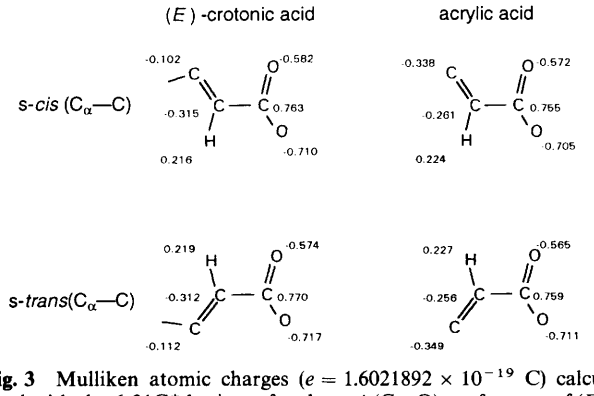

Fig. 3 Mulliken atomic charges ($e = 1.6021892 \times 10^{-19}$ C) calculated with the 6-31G* basis set for the s-*cis*(C—O) conformers of (*E*)-crotonic and acrylic[9] acids

dipoles[29] and steric repulsions between H_α or H_β and the oxygen atoms of the carboxylic group. The E-tt conformation [the second possible *trans*(C—O) structure] was found to correspond to a conformational transition state (saddle point) separating the two equivalent-by-symmetry non-planar conformers, herein referred to as E-np (see Fig. 1). The calculated energy difference between the E-np forms and the planar E-tt structure is 1.56 kJ mol^{-1}.

By comparing the molecular geometries of the E-tc and E-np forms with those of the two s-*cis*(C—O) conformers (E-cc and E-ct) the following conclusions can also be drawn:

(i) The O—H bond is shorter in the E-tc and E-np conformers than in the two s-*cis*(C—O) conformers. This is a direct consequence of the presence in these latter conformers of the abovementioned C=O···O—H through-space field interaction which leads to an increase in the O—H bond length by inducing an electronic charge migration from the overlap O—H region towards the —O— atom;

(ii) The C=O and C—O bond lengths are, respectively, smaller and larger than in the two s-*cis*(C—O) conformers, indicating that the mesomerism within the carboxylate group has a reduced importance when the O=C—O—H axis assumes the s-*trans* conformation (as in E-tc) or a conformation close to this (as in E-np);

(iii) In both the high energy forms, the OH···CRH=CH repulsive steric interactions are very important, leading to very large C—C—O, C—O—H and H—C—C angles. Obviously, these interactions are much stronger in the case of the E-np form, where the CRH=CH moiety is close to the sterically more important —O— atom. Indeed, such interactions are strong enough to put the energy of the planar E-tt conformation [corresponding to a saddle point in the PES of (*E*)-crotonic acid] above that of the non-planar structure corresponding to the stable form E-np, despite the mesomerism involving the C=C—C=O moiety and/or the carboxylic group cannot operate so efficiently for non-planar structures as for planar conformations;

(iv) The OH···CRH=CH steric interactions are also responsible, at least in part, for the presence of a longer C_α—C bond in both E-tc and E-np conformers, though this result may also be partially due to a reduced importance in these forms of the mesomerism involving the C=C—C=O moiety.

(*Z*)-*Crotonic Acid*

Table 1 presents the calculated molecular geometries, rotational constants and dipole moments for the three possible conformers of (*Z*)-crotonic acid (see Fig. 1). The energy of the most stable conformer of this compound (Z-cc in Fig. 1) is *ca.* 10.5 kJ mol^{-1} higher than that of the most stable form of (*E*)-crotonic acid (E-cc). This increase in energy in going from E-cc to Z-cc can be ascribed to a reduced methyl–carbonyl distance in the latter molecule, which leads to steric strain. Indeed, this conclusion is reinforced by the relative values of the C—C=O, C=C_α—C, C—C_β=C and $H_{(10)}$—C—C bond angles in the two molecules, which are all larger in Z-cc due to the methyl–carbonyl steric repulsion. Apart from the changes observed in the above bond angles (and in those which must adjust to compensate these changes), the structural differences between E-cc and Z-cc are not significant.

The internal rotation about the C_α—C bond in (*Z*)-crotonic acid, as for (*E*)-crotonic acid, gives two different conformers: the lowest energy form mentioned above (Z-cc) and the Z-ct conformer (7 kJ mol^{-1} less stable than the Z-cc conformer), which have C=C—C=O dihedral angles equal to 0° and 180°, respectively. On the other hand, in contrast to (*E*)-crotonic acid, (*Z*)-crotonic acid possesses only one stable non-s-*cis*(C—O) conformation. In fact, in this latter com-

pound, besides the two s-*cis*(C—O) forms (Z-cc and Z-ct) only the Z-tc conformer exists, where the C=C—C=O axis assumes the s-*cis* conformation and the O=C—O—H axis is in the s-*trans* conformation (see Fig. 1). This different conformational behaviour found for (*Z*)- and (*E*)-crotonic acids can be easily understood considering the relative importance of the steric interactions involving the β-carbon substituent *cis* to the C(=O)OH fragment in the two molecules. When compared with the H atom [the β-carbon substituent *cis* to the C(=O)OH fragment in (*E*)-crotonic acid], the bigger methyl substituent present in (*Z*)-crotonic acid leads to stronger steric repulsions with either the carbonyl oxygen atom (in s-*cis* forms) or hydroxy group (in s-*trans* conformations). This increase of energy due to the $H \rightarrow CH_3$ substitution is, however, particularly critical for the s-*trans* conformation, where the steric interaction involves the sterically much more important OH group.

The conformation dependence of the geometrical parameters in (*Z*)-crotonic acid follows the same patterns found in (*E*)-crotonic acid, and can be ascribed to the same general effects discussed above. However, in general the changes in bond angles are more pronounced owing to the increased importance of steric effects in this molecule (see, for instance the relative values of C—C=O and C—C—O angles in E-cc *vs.* E-ct and in *Z*-cc *vs.* *Z*-ct, shown in Table 1).

Finally, it is also noteworthy that the calculated electric dipole moments of the various conformers of (*Z*)-crotonic acid are systematically smaller than those of (*E*)-crotonic acid (see Table 1). This result can be understood considering the closer proximity of the positively charged β-carbon methyl substituent of the negatively charged oxygen atoms in (*Z*)-crotonic acid, and have potential applications to distinguish the two molecules in appropriate chemical environments (*e.g.* solvents polarity).

Vibrational Studies

UV-induced Isomerization Reactions and the Spectra of the Individual Conformers

The IR spectra of (*E*)-crotonic acid isolated in Ar and Kr matrices are essentially the same; both the observed frequencies and intensities do not differ by more than 0.5%. Thus, the following discussion will focus on the results obtained in the Ar matrix.

The IR spectrum of (*E*)-crotonic acid trapped in an Ar matrix deposited at 18 K is shown in Fig. 4. In addition to the bands due to the monomers, the spectrum contains some low intensity bands due to traces of cyclic dimers initially present in the jet used to prepare the samples, which could be identified by recording the spectra with different matrix : solute ratios.

Under irradiation with UV light of decreasing wavelength, a noticeable redistribution of band intensities begins to take place at *ca.* 262 nm (filter 250FS10-50; peak transmission 17% at 262.3 nm; bandwidth 10.3 nm) indicating that UV-induced rotamerization reactions involving the conversion between those conformers of (*E*)-crotonic acid which are initially present in the sample are taking place. In addition, new bands appear in the spectrum, testifying the appearance of new species. Under irradiation in the 243–253 nm region (filter 240FS10-50; peak transmission 24% at 243 nm; bandwidth 9.4 nm), the changes were found to be similar, but for wavelengths smaller than 243 nm (non-filtered UV light was used) bands due to CO, CO_2 and H_2O appear in the spectrum, indicating the beginning of the acid photodissociation processes. Fig. 5 shows the IR spectra obtained after irradiation in the 243–253 nm region (in hexane solution at room temperature, the λ_{max} of the (*E*)-crotonic acid ethylenic π–π^*

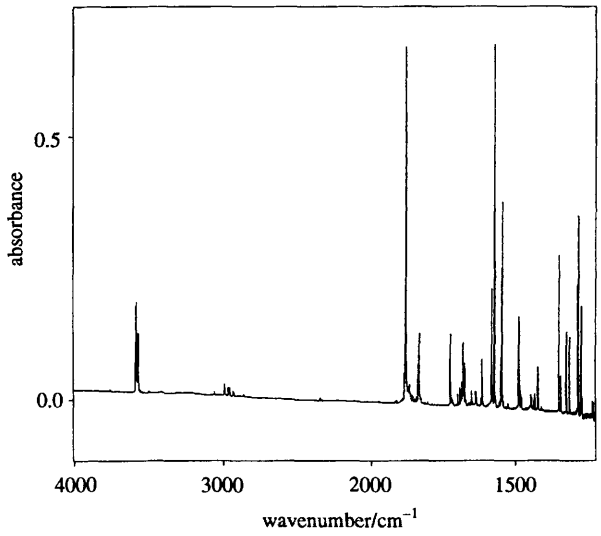

Fig. 4 IR spectrum of (*E*)-crotonic acid isolated in an argon matrix deposited at 18 K

absorption band is 219 nm, and the half bandwidth is 18 nm; thus, the irradiation was carried out in the long-wavelength wing of the absorption band) and after irradiation by non-filtered light. The corresponding differential spectra are shown in Fig. 6.

The observed redistribution of the intensities of the precursor bands already present in the spectrum (two sets of bands showing different behaviour upon irradiation were found) must be due to a rotamerization reaction between the two lower energy E-cc and E-ct conformers, since the two forms are significantly populated at the deposition temperature. Indeed, as indicated by the calculations (see Table 1), the relative energy of the remaining conformers of (*E*)-crotonic acid (the E-tc and E-np forms) are high enough to avoid this form being significantly populated even at considerably high temperatures. The comparison between the deconvoluted spectra of the two forms of (*E*)-crotonic acid initially present in the sample obtained from the difference spectra (irradiated sample – non-irradiated sample) shown in Fig. 6 and the calculated spectra for the two most stable conformers of (*E*)-crotonic acid (see Fig. 7) shows that the downwards bands can be ascribed to the E-cc form. Thus, it can be concluded that irradiation promotes E-cc → E-ct isomerization.

An estimation of the relative population of the E-cc and E-ct conformers in the non-annealed sample could be carried out by taking into consideration the data shown in Fig. 8.

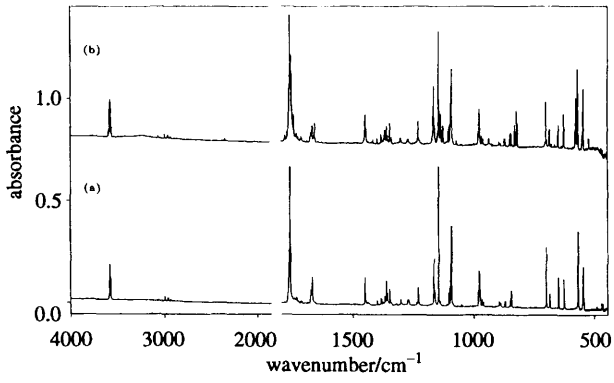

Fig. 5 IR spectra of a sample of (*E*)-crotonic acid isolated in an argon matrix (a) after UV irradiation for *ca.* 2 h in the 240–250 nm region (changes in the spectrum are close to saturation) and (b) after irradiation by non-filtered UV light

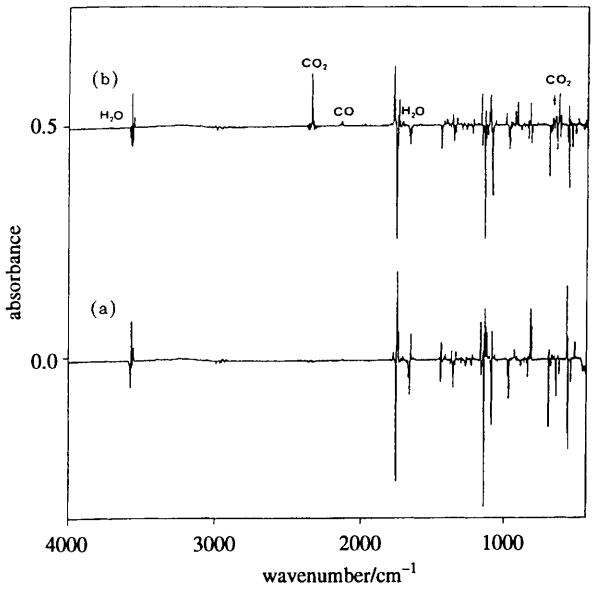

Fig. 6 Difference spectra obtained by subtracting the spectrum of the non-irradiated sample from: (a) the spectrum obtained after UV irradiation in the 240–250 nm region; (b) the spectrum obtained after irradiation by non-filtered UV light

Based on the different behaviour of the various bands observed in the ν(O—H) stretching spectral region upon irradiation at 243–253 nm and by non-filtered light, the bands at 3579.3 and 3577.3 cm^{-1} could be ascribed to E-cc, while the 3585.7 and 3566.8 cm^{-1} bands were ascribed to E-ct. Assuming equal ν(O—H) integral absorption coefficients in these two conformers (as indicated by the calculations), an E-cc : E-ct population ratio equal to 1 : 0.65 could be estimated from the experimental data. This result is in fairly good agreement with the predicted relative population at room temperature obtained from the calculated relative conformational energy (1 : 0.35). On the other hand, since the annealing of the matrices up to 32 K does not change the spectra of either irradiated or non-irradiated samples, it can be concluded that the barrier for internal rotation about the C_α—C bond must be larger than 12 kJ mol^{-1}.[32] This lower limit also agrees fairly well with the previously found gas-phase value, obtained from microwave spectroscopy for the acrylic acid monomer (16.0 ± 6.0 kJ mol^{-1} [33]).

The appearance of new bands in the spectra obtained after UV irradiation of the sample indicates, as referred to above, the photochemical production of new species. As two groups of bands, exhibiting different intensity dependence on the irradiation wavelength, were found, it can be concluded that two different molecules are formed. Indeed, the comparison of the deconvoluted IR spectra of the individual experimentally observed molecules with the 6-31G* calculated spectra clearly shows that these molecules correspond to the two s-*cis*(C—O) conformers of (*Z*)-crotonic acid (Z-cc and Z-ct; see Fig. 9). Note, the (*E*)-crotonic acid → (*Z*)-crotonic acid isomerization is both faster and more pronounced than the C_α—C rotamerization proccess discussed above that promotes E-cc → *E*-ct conversion. Though volume restrictions imposed by the matrix or relative masses of the rotating group may also explain this observation, it is more probable that the double bond character of the C=C bond strongly reduces upon electronic excitation and, consequently, its associated energy barrier to internal rotation becomes lower in the excited state than that associated with the C_α—C bond. The E-cc : Z-cc relative population present in the original gaseous mixture, estimated from the data shown in Fig. 8a [obtained assuming equal ν(O—H) integral absorption coefficients in both forms] is 1 : 0.05; a result which is in fairly good agreement with the predicted value at room temperature (1 : 0.02)

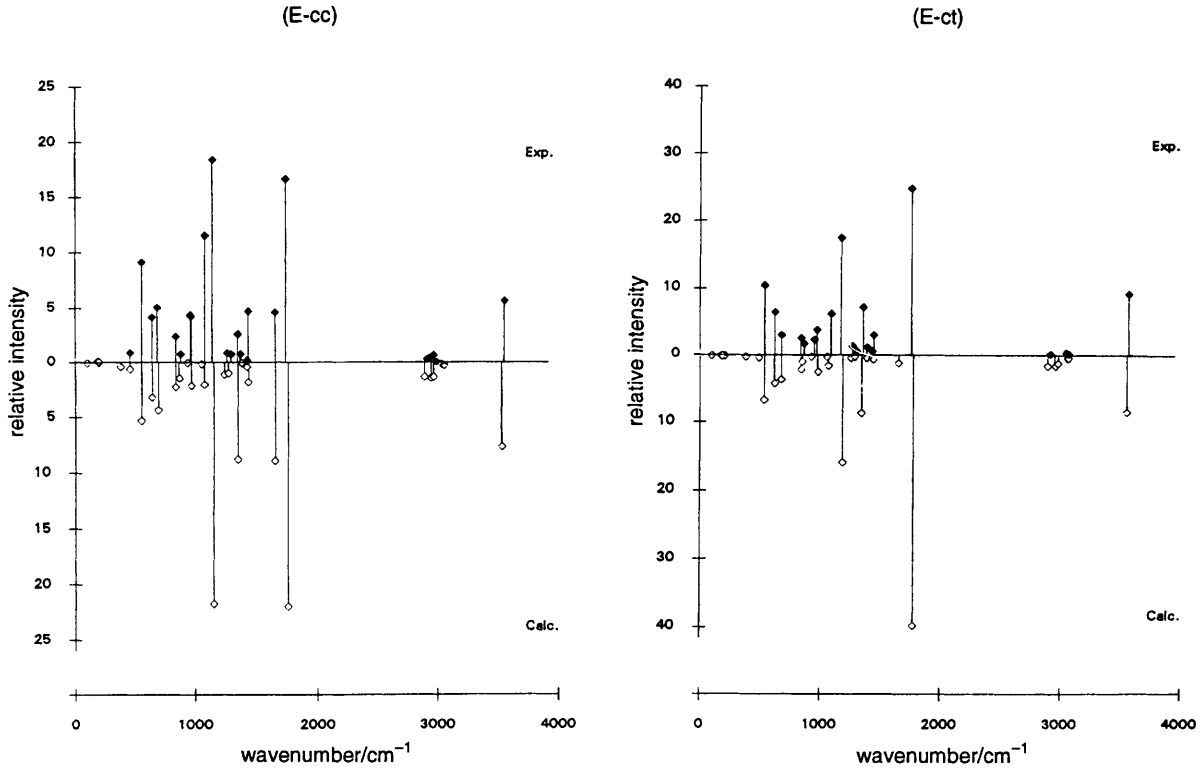

Fig. 7 Deconvoluted experimental IR spectra and SCF-HF/6-31G* calculated spectra of the E-cc and E-ct conformers of (*E*)-crotonic acid. Experimental relative intensities correspond to intensities normalized to the total intensity of all observed bands ascribed to a given conformer ($I = 100\ I^{obs}/\sum_{i=1,n} I_i^{obs}$); calculated relative intensities are normalized to the total calculated intensity of all bands which have an experimentally observed counterpart.

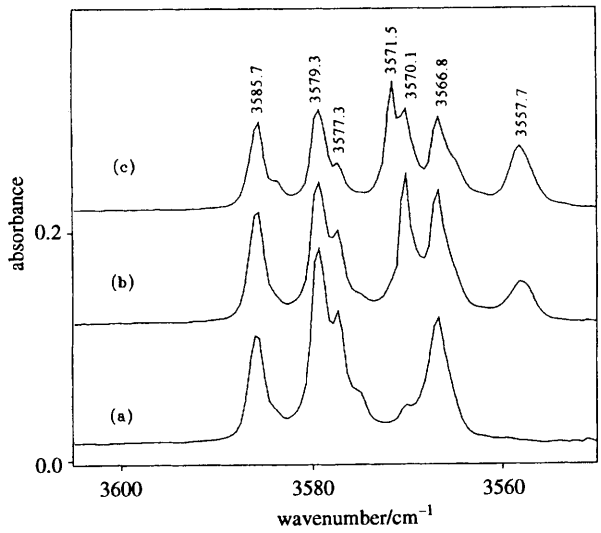

Fig. 8 ν(O—H) stretching IR spectral region: (a) non-irradiated sample; (b) after irradiation in the 243–253 nm region both the 3579.3 and 3577.3 cm^{-1} bands (E-cc) decrease in intensity, while bands at 3570.1 (Z-cc) and 3557.7 cm^{-1} (Z-ct) become more intense and bands at 3585.7 and 3566.8 cm^{-1} (E-ct) do not change appreciably; (c) after irradiation with non-filtered light all bands decrease in intensity, while a new band at 3571.5 cm^{-1} (photodecomposition product) appears in the spectrum. This different behaviour compared with the irradition processes was taken as a base for spectral deconvolution.

obtained from the calculated relative energies of the two molecules.

The experimental and 6-31G* calculated wavenumbers and intensities, as well as the potential-energy distribution (PED) for the observed conformers of both (*E*)- and (*Z*)-crotonic acids are shown in Tables 2–5. Tables 6 and 7 present the calculated values obtained for the higher energy forms (E-tc, E-np and Z-tc). These Tables also include the wavenumbers obtained with the scaled force fields. These latter show a general agreement with the experimental values to within 2% for the experimentally observed conformers (see also Fig. 10).

All the studied conformers except for E-np belong to the C_S point group and thus, their 30 normal modes span the irreducible representations, 20 A′ + 10 A″. Form E-np belongs to the C_1 point group and all their vibrations belong to the totally symmetric representation. Table 8 shows the local C_S symmetry coordinates used in the normal coordinate analysis.

Most of the observed IR bands ascribable to individual conformers appear as close doublets resulting from molecules trapped in different matrix environments (some bands show a more complex structure). Thus, for these cases, in order to make a more direct comparison with the calculated values, the gravity centres of the experimental bands were obtained [$\nu^{gc} = \sum_i(\nu^{obs} I^{obs})/\sum_i I^{obs}$; $I^t = \sum_i^{obs}$, with i being the number of components resulting from matrix site effects].

(*E*)-*Crotonic Acid*. The experimental IR spectra of the two individual conformers (E-cc and E-ct) are characterized by the systematic appearance of the bands grouped as doublets originating from two different sets of molecules trapped in two different matrix environments. In addition, some vibrations give rise to additional bands which can be ascribed to Fermi resonance interactions.

In the E-cc spectrum, both the ν(C=O) and ν(C=C) vibrations appear as triplets [ν(C=O): 1758.8, 1756.5, 1755.1 cm^{-1}; ν(C=C): 1671.9, 1669.6, 1663.9 cm^{-1}]. Considering the relative intensities of the observed components, the pairs of bands at 1758.8/1755.1 cm^{-1} and 1671.9/1669.6 cm^{-1} are assigned to ν(C=O) and ν(C=C) of one set of molecules [whose vibrations are involved in Fermi resonance, most probably with the 1st overtones of ν(C$_\alpha$—C) and γ(C$_\beta$—H)

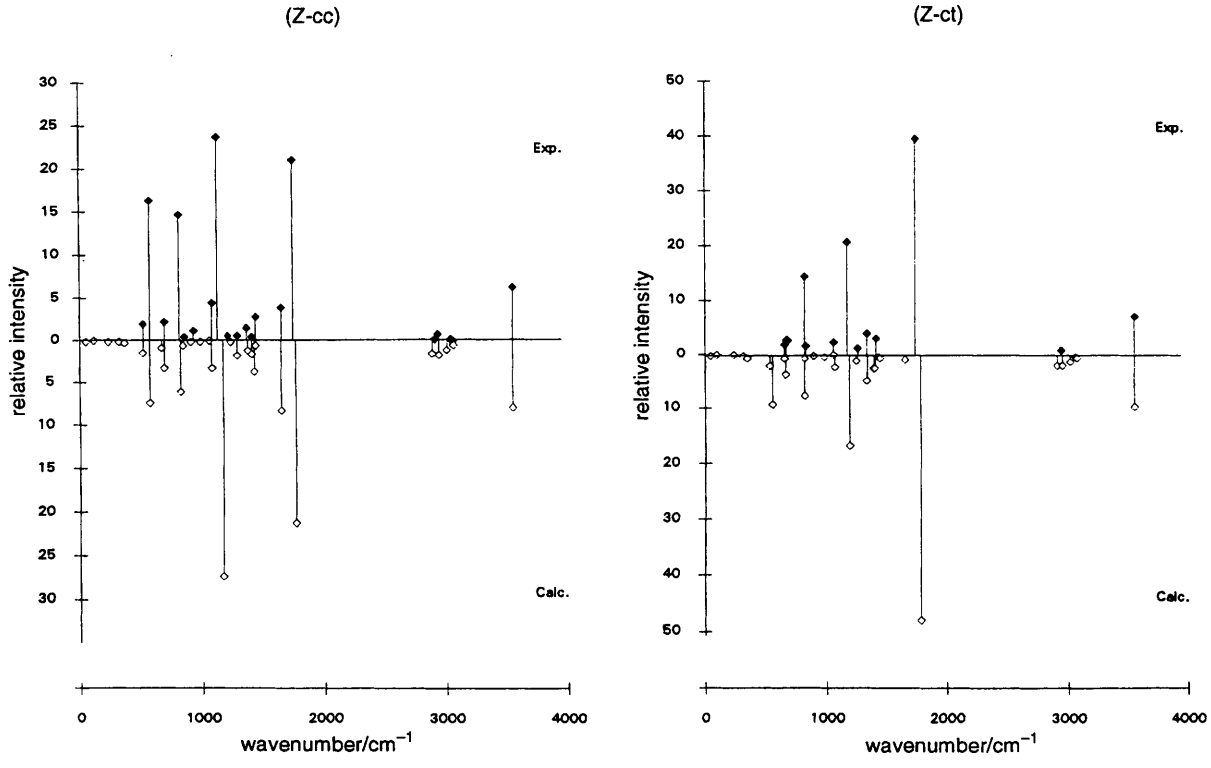

Fig. 9 Deconvoluted IR experimental spectra and SCF-HF/6-31G* calculated spectra of the Z-cc and Z-ct conformers of (*Z*)-crotonic acid. Experimental relative intensities correspond to intensities normalized to the total intensity of all observed bands ascribed to a given conformer ($I = 100\ I^{obs}/\sum_{i=1,n} I_i^{obs}$); calculated relative intensities are normalized to the total calculated intensity of all bands which have an experimentally observed counterpart.

Table 2 Experimental and calculated vibrational wavenumbers (cm^{-1}) and intensities for (*E*)-crotonic acid (E-cc form)

		exp. (IR, Ar matrix)				calc. (6-31G*)			
approximate description	symmetry	ν	I	ν^{gc} [a]	I^{total} [b]	ν	I	ν^{scaled} [c]	PED[d]
ν(O—H)	A′	3579.3	2.9	3578.2	5.5	4060	7.7	3562	s_1[100]
		3577.3	2.1						
		3575.3	0.5						
ν(C_α—H)	A′	no				3388	0.4	3074	s_2[99]
ν(C_β—H)	A′	3020.4	<0.1	3015.4[e]	<0.1	3369	0.2	3057	s_3[99]
		3010.3	<0.1						
$\nu(CH_3)_{as}$	A′	2990.7	0.4	2990.0[e]	0.6	3288	1.3	2985	s_4[97]
		2988.6	0.2						
$\nu(CH_3)_{as}$	A″	2963.5	0.2	2957.5[e]	0.4	3254	1.4	2967	s_{21}[101]
		2953.3	0.2						
$\nu(CH_3)_s$	A′	2931.4	0.2	2929.3[e]	0.3	3202	1.4	2907	s_5[98]
		2925.0	0.1						
ν(C═O)	A′	1758.8	4.0	1756.6	16.4	2007	22.1	1774	s_6[90]
		1756.5	7.5						
		1755.1	4.9						
ν(C═C)	A′	1671.9	0.8	1667.0	4.5	1883	9.0	1666	s_7[72] + s_{12}[12] + s_{11}[10]
		1669.6	1.3						
		1663.9	2.4						
$\delta(CH_3)_{as}$	A′	1449.7	2.1	1448.5	4.6	1629	1.9	1445	s_8[92]
		1447.6	2.5						
$\delta(CH_3)_{as}$	A″	1435.8	0.2	1435.8	0.2	1623	0.4	1434	s_{22}[94]
$\delta(CH_3)_s$	A′	1379.1	0.5	1377.4	0.8	1565	0.2	1389	s_9[104]
		1374.6	0.3						
ν(C—O) + δ(C—O—H)	A′	1360.1	1.9	1358.9	2.6	1532	8.8	1360	s_{10}[26] + s_{16}[17] + s_{13}[16] + s_{11}[15] + s_{17}[13]
		1355.5	0.7						
δ(C_β—H)	A′	1319.9	0.2	1306.2	0.7	1445	1.0	1284	s_{12}[64] + s_7[13]
		1300.7	0.5						
δ(C_α—H)	A′	1272.8	0.5	1271.3[e]	0.9	1412	1.1	1255	s_{11}[41] + s_{13}[33]
		1269.4	0.4						
δ(C—O—H) + ν(C—O)	A′	1236.2	0.3	1147.1[e]	18.0	1312	21.8	1169	s_{13}[32] + S_{10}[46]
		1233.0	0.3						
		1144.6	11.8						
		1143.0	5.6						
$\gamma(CH_3)$	A′	1093.5	4.9	1091.5	11.3	1216	2.1	1085	s_{14}[31] + s_{15}[26] + s_{11}[14]
		1089.9	6.4						
$\gamma(CH_3)$ + γ($C_{\beta'}$—H)	A″	no				1203	0.2	1064	s_{23}[44] + s_{25}[61]
γ(C_α—H)	A″	979.2	1.3	975.5[e]	4.2	1107	2.2	979	s_{24}[82] + s_{26}[17]
		973.9	2.9						
ν(C—C)	A′	972.7	2.8	971.9[e]	4.3	1058	0.1	948	s_{15}[37] + s_{16}[26] + s_{10}[10]
		970.5	1.5						
ν(C_α—C)	A′	892.5	0.4	889.6	0.8	979	1.5	879	s_{16}[24] + s_{14}[36] + s_{19}[13] + s_{12}[10] + s_{15}[10]
		886.7	0.4						
γ(C_β—H) + $\gamma(CH_3)$	A″	842.2	1.2	841.2	2.3	958	2.4	847	s_{25}[38] + s_{23}[49] + s_{11}[11]
		840.1	1.1						
γ(C═O)	A″	698.6	5.0	698.6	5.0	793	4.4	702	s_{26}[70] + s_{24}[13]
δ(O═C—O)	A′	648.9	1.5	647.7	4.0	718	3.3	651	s_{17}[58] + s_{10}[10]
		647.0	2.5						
τ(C—O)	A″	567.0	2.8	565.6	8.9	638	5.4	565	s_{27}[98]
		565.0	6.1						
δ(C—C═O)	A′	468.7	0.5	466.2	0.9	504	0.7	465	s_{18}[52] + s_{17}[16] + s_{20}[10]
		463.1	0.4						
δ(C—C_β═C)	A′	no				420	0.4	391	s_{20}[46] + s_{16}[14]
τ(C═C)	A″	no				222	<0.1	198	s_{29}[100] + s_{26}[11]
τ(C—C)	A″	no				208	<0.1	186	s_{28}[76] + s_{30}[17]
δ(C═C_α—C)	A′	no				201	0.1	201	s_{19}[57] + s_{20}[27] + s_{18}[24]
τ(C_α—C)	A″	no				110	0.1	100	s_{30}[86] + s_{28}[17]

Vibrations: ν, stretching; δ, bending; ω, wagging; γ, rocking; τ, torsion. no, not observed; s, symmetric; as, asymmetric. See Table 8 for definition of coordinates. Experimental intensities are normalized to the total intensity of all observed bands ($I = 100\, I^{obs}/\sum_{i=1,n} I_i^{obs}$, where n is the number of observed IR bands ascribed to the conformer). Calculated intensities are normalized to the total calculated intensity of all bands which have an experimentally observed counterpart. The non-normalized *ab initio* intensities (km mol^{-1}) can be obtained by multiplying the values presented in the Table by 16.82. [a] ν^{gc} correspond to the wavenumbers of the gravity centres of the groups of bands ascribed to the same normal mode; they are calculated as $\nu^{gc} = \sum_i(\nu^{obs} I^{obs})/\sum_i I^{obs}$, where i is the number of total components of the group of bands. [b] I^{total} is the total intensity of the bands ascribed to the same normal mode. [c] The resulting scaled C—H stretching wavenumbers were found to be considerably underestimated (error ≈ 3–4%). An additional correction factor (1.033) was then applied specifically to these vibrations, leading to a reduced error of less than 1%. Such an additional correction factor was obtained by linear regression, constrained by assuming a zero intercept and performed using all observed/scaled ν(C—H) wavenumbers for all observed conformers. [d] PEDs < 10% are not presented in the Table. [e] Value not used in the force-field scaling.

Table 3 Experimental and calculated vibrational wavenumbers (cm^{-1}) and intensities for (*E*)-crotonic acid (E-ct form)

		exp. (IR, Ar matrix)				calc. (6-31G*)			
approximate description	symmetry	ν	I	$\nu^{sc\ a}$	$I^{total\ b}$	ν	I	$\nu^{scaled\ c}$	PED[d]
ν(O—H)	A′	3585.7	4.2	3575.5	9.1	4064	8.4	3565	s_1[100]
		3566.8	4.9						
ν(C_α—H)	A′	3080.7	0.1	3080.7	0.1	3389	0.4	3075	s_2[98]
ν(C_β—H)	A′	3061.6	0.1	3060.3[e]	0.4	3374	0.5	3062	s_3[98]
		3059.9	0.3						
$\nu(CH_3)_{as}$	A′	no				3289	1.3	2986	s_4[97]
$\nu(CH_3)_{as}$	A″	no				3253	1.6	2966	s_{21}[101]
$\nu(CH_3)_s$	A′	2926.7	0.2	2926.7[e]	0.2	3202	1.6	2907	s_5[97]
ν(C═O)	A′	1764.5	2.7	1757.6	24.4	2022	39.8	1786	s_6[87]
		1756.7	21.7						
ν(C═C)	A′	no				1877	1.3	1661	s_7[71] + s_{12}[12]
$\delta(CH_3)_{as}$	A′	1446.4	2.9	1446.4	2.9	1628	0.8	1444	s_8[94]
$\delta(CH_3)_{as}$	A″	1441.8	0.5	1441.8	0.5	1623	0.4	1434	s_{22}[94]
$\delta(CH_3)_s$	A′	1397.2	1.0	1397.2[e]	1.0	1566	0.5	1390	s_9[103]
ν(C—O) + δ(C—O—H)	A′	1382.3	1.6	1359.8[e]	7.1	1523	8.6	1352	s_{10}[31] + s_{16}[23] + s_{13}[22] + s_{17}[17]
		1365.9	1.8						
		1352.0	0.4						
		1346.6	3.3						
δ(C_β—H)	A′	1308.0	0.3	1307.6	0.5	1453	0.3	1291	s_{12}[62] + s_7[14]
		1307.0	0.2						
δ(C_α—H)	A′	1268.0	1.2	1268.0	1.2	1423	0.5	1265	s_{11}[70] + s_{12}[13]
δ(C—O—H) + ν(C—O)	A′	1229.0	3.9	1178.0	17.0	1344	16.0	1196	s_{13}[61] + s_{10}[25]
		1163.9	9.7						
		1159.7	3.4						
$\gamma(CH_3)$ + ν(C—C)	A′	1101.9	2.5	1098.9	6.1	1208	1.6	1078	s_{14}[32] + s_{15}[36]
		1096.9	3.6						
$\gamma(CH_3)$ + γ(C_β—H)	A″	no				1199	0.2	1060	s_{23}[47] + s_{25}[57]
γ(C_α—H)	A″	976.8	3.7	976.8	3.7	1112	2.6	983	s_{24}[47] + s_{23}[16] + s_{25}[14]
ν(C—C) + $\gamma(CH_3)$	A′	962.8	1.4	961.0	2.2	1049	0.3	939	s_{15}[36] + s_{14}[20] + s_{10}[13] + s_{16}[12]
		957.8	0.8						
ν(C_α—C)	A′	870.2	1.1	867.8	2.5	960	1.1	862	s_{16}[24] + s_{14}[24] + s_{10}[23] + s_{19}[10]
		865.9	1.4						
γ(C_β—H) + $\gamma(CH_3)$	A″	845.8	1.9	845.8	1.9	959	2.2	848	s_{25}[40] + s_{23}[45]
γ(C═O)	A″	683.9	2.9	683.9	2.9	773	3.8	685	s_{26}[54] + s_{24}[21] + s_{23}[12]
δ(O═C—O)	A′	624.6	6.2	624.6	6.2	689	4.3	626	s_{17}[71] + s_{13}[13] + s_{19}[13]
τ(C—O)	A″	548.0	1.9	543.9	10.1	614	6.7	544	s_{27}[102]
		542.9	8.2						
δ(C—C═O)	A′	no				541	0.4	497	s_{18}[54] + s_{16}[11] + s_{19}[10]
δ(C—C_β═C)	A′	no				410	0.3	383	s_{20}[50] + s_{18}[14] + s_{16}[11]
τ(C═C)	A″	no				219	<0.1	195	s_{29}[91] + S_{26}[12]
δ(C═C_α—C)	A′	no				209	0.1	207	s_{19}[55] + s_{20}[25] + s_{18}[22]
τ(C—C)	A″	no				207	<0.1	184	s_{28}[76] + s_{30}[15]
τ(C_α—C)	A″	no				109	<0.1	98	s_{30}[83] + s_{28}[16]

See Table 2 for all definitions except for non-normalized *ab initio* intensities (km mol^{-1}) which can be obtained by multiplying the values in the Table by 15.55.

+ $\gamma(CH_3)$, respectively], while bands at 1756.5 and 1663.9 cm^{-1} are assigned to the same vibrations belonging to a second set of molecules, in a different matrix site, which are not interacting by Fermi resonance. In turn, the presence of four bands ascribable to the δ(COH) + ν(C—O) mode may also be explained assuming the participation of this vibration in a Fermi resonance interaction with the 1st overtone of the δ(O═C—O) mode, in the two non-equivalent sets of molecules. However, the precise identification of the components of each doublet cannot be made, since it is apparent that the interactions with the matrix, in the two matrix sites observed, affect the intensities of this vibration in a different way. Indeed, in this case, the sum of the intensities of the Fermi doublets originated in the two non-equivalent sets of molecules are considerably different.

In the case of the E-ct conformer, similar Fermi resonance interactions involving the δ(COH) + ν(C—O) and ν(C—O) + δ(COH) vibrations seem also to occur. As was found for the E-cc form, the relative intensities of the various band components of the observed E-ct multiplets also point to identical populations of molecules and similar intensity perturbations owing to interactions with the matrix in the two observed matrix sites. Thus, the pairs of bands at 1382.3/1365.9 cm^{-1}, 1352.0/1346.6 cm^{-1} [ν(C—O) + δ(COH)] and 1229.0/1159.7 cm^{-1} [δ(COH) + ν(C—O)] are easily assigned to Fermi resonance doublets originating in molecules in one particular matrix site. The band at 1163.9 cm^{-1} corresponds to the 'pure' δ(COH) + ν(C—O) mode of these molecules in the second matrix site (differing from that associated with the Fermi doublet observed at 1229.0/1159.7 cm^{-1}).

It is important to note that the involvement of δ(COH) + ν(C—O), ν(C—O) + δ(COH), ν(C═C) and ν(C═O) fundamentals in Fermi resonance interactions has already been observed previously for other monomeric carboxylic acids (in particular acrylic acid) isolated in noble gas matrices.[9,19,29]

Also, as has been found for other monomeric carboxylic acids isolated in noble gas matrices,[9,19,29] some of the ν(CH) vibrations could not been observed in the IR spectra of (*E*)-crotonic acid (see Tables 2 and 3). This is, however, due to

Table 4 Experimental and calculated vibrational wavenumbers (cm^{-1}) and intensities for (*Z*)-crotonic acid (Z-cc form)

		exp. (IR, Ar matrix)				calc. (6-31G*)			
approximate description	symmetry	ν	I	$\nu^{gc\,a}$	$I^{total\,b}$	ν	I	$\nu^{scaled\,c}$	PED[d]
ν(O—H)	A′	3570.1	6.1	3570.1	6.1	4062	8.0	3564	s_1[100]
ν(C_α—H)	A′	no				3391	0.6	3077	s_2[95]
$\nu(CH_3)_{as}$	A′	no				3373	0.1	3061	s_4[83] + s_5[12]
ν(C_β—H)	A′	3058.1	0.2	3058.1[e]	0.2	3330	1.2	3022	s_3[94]
$\nu(CH_3)_{as}$	A″	2955.1	0.1	2947.7[e]	0.7	3243	1.7	2957	s_{21}[101]
		2945.9	0.6						
$\nu(CH_3)_s$	A′	2921.9	0.2	2921.9[e]	0.2	3200	1.6	2906	s_5[88] + s_4[15]
ν(C=O)	A′	1752.5	11.8	1751.3	20.6	2006	21.2	1773	s_6[90]
		1749.6	8.8						
ν(C=C)	A′	1653.7	3.7	1653.7	3.7	1873	8.3	1657	s_7[77]
$\delta(CH_3)_{as}$	A″	no				1641	0.5	1450	s_{22}[89]
$\delta(CH_3)_{as}$	A′	1444.4	2.7	1444.4	2.7	1626	3.7	1442	s_8[72] + s_{11}[10]
δ(C_β—H)	A′	1419.8	0.4	1419.8	0.4	1595	1.6	1415	s_{12}[24] + s_8[28] + s_{11}[23] + s_9[10]
$\delta(CH_3)_s$	A′	1369.5	1.4	1369.5	1.4	1552	1.2	1377	s_9[92]
δ(C—O—H) + ν(C—O)	A′	1298.3	0.5	1298.3	0.5	1462	1.8	1299	s_{13}[39] + s_{10}[15] + s_{12}[14] + s_{17}[11]
δ(C_α—H)	A′	1221.7	0.6	1221.7	0.6	1392	0.2	1238	s_{11}[32] + s_{12}[30]
ν(C—O) + δ(C—O—H)	A′	1148.1	1.9	1135.0[e]	23.2	1316	27.3	1172	s_{10}[53] + s_{13}[37]
		1141.2	6.1						
		1135.4	5.3						
		1134.4	3.5						
		1126.2	3.2						
		1124.5	3.2						
$\gamma(CH_3)$	A′	1088.4	4.4	1088.4	4.4	1218	3.2	1086	s_{14}[43] + s_{11}[14] + s_{19}[14] + s_{15}[11]
$\gamma(CH_3)$ + γ(C_β—H)	A″	no				1205	<0.1	1066	s_{23}[42] + s_{25}[64] + s_{29}[14]
γ(C_α—H)	A″	no				1116	0.2	987	s_{24}[43] + s_{23}[27] + s_{25}[16]
ν(C—C)	A′	933.9	1.1	933.9	1.1	1015	0.1	910	s_{15}[34] + s_{14}[26] + s_{16}[18]
ν(C_α—C)	A′	861.9	0.4	861.9	0.4	939	0.7	843	s_{16}[28] + s_{15}[34] + s_{19}[15] + s_{18}[10]
γ(C_β—H) + $\gamma(CH_3)$	A″	820.6	2.2	818.3	14.3	932	6.1	824	s_{25}[44] + s_{23}[21] + s_{26}[21] + s_{24}[10]
		819.6	6.7						
		817.7	0.8						
		815.3	4.6						
δ(O=C—O)	A′	702.9	0.8	698.1	2.1	768	3.3	695	s_{17}[31] + s_{19}[24] + s_{20}[17] + s_{10}[12] + s_{18}[11] + s_{14}[10]
		695.2	1.3						
γ(C=O)	A″	no				758	0.8	671	s_{26}[47] + s_{24}[30] + s_{25}[11]
τ(C—O)	A″	575.8	4.7	574.4	16.0	644	7.5	571	s_{27}[91]
		574.2	9.4						
		571.8	1.9						
δ(C—C_β=C)	A′	520.0	1.9	520.0	1.9	566	1.4	519	s_{20}[15] + s_{17}[50] + s_6[18]
δ(C—C=O)	A′	no				392	0.3	367	s_{18}[60] + s_{20}[58]
τ(C=C)	A″	no				360	0.1	320	s_{29}[77] + s_{26}[20]
δ(C=C_α—C)	A′	no				238	0.2	233	s_{19}[53] + s_{18}[15]
τ(C—C)	A″	no				123	<0.1	111	s_{28}[103]
τ(C_α—C)	A″	no				58	0.1	54	s_{30}[99]

See Table 2 for all definitions except for non-normalized *ab initio* intensities (km mol^{-1}) which can be obtained by multiplying the values in the Table by 16.19.

the very low intensities of these modes in the IR, as can be inferred from the corresponding calculated intensities shown in Tables 2 and 3. In turn, their Raman activities were predicted to be very large [the 6-31G* calculations predict that, together with the ν(O—H) and ν(C=C) modes, the ν(CH) vibrations are those giving rise to the most intense Raman bands], and in the Raman spectra of room temperature crystalline (*E*)-crotonic acid prominent bands appear at 3058, 3039, 2978, 2957 and 2925 cm^{-1}, which can be ascribed to ν(C_α—H), ν(C_β—H), $\nu(CH_3)_{as}$ (a′), $\nu(CH_3)_{as}$ (a″) and $\nu(CH_3)_s$, respectively.[34]

As noted in our previous study on acrylic acid,[9] the predicted (scaled) ν(CH) wavenumbers are somewhat lower than those observed (error ≈ 3–4%). This may be only due to the exceptionally large anharmonicity usually exhibited by these vibrations or result from intermolecular interactions (either between the molecules of the acid, in the crystal or between crotonic acid and the matrix environment, in the matrix-isolated situation). In addition, the worse agreement between predicted (scaled) and experimental wavenumbers may also be a consequence, at least in part, of the involvement of the ν(CH) fundamentals in Fermi resonance interactions, as suggested by the appearance in the ν(CH) spectral region of a number of additional lower intensity bands. However, in order to reach a better agreement between the observed and calculated (scaled) wavenumbers, an additional correction factor to the scaled wavenumbers was determined by linear regression constrained by assuming a zero intercept and performed using all observed/scaled ν(CH) wavenumbers for all observed conformers. After this extra correction, the calcu-

Table 5 Experimental and calculated vibrational wavenumbers (cm^{-1}) and intensities for (*Z*)-crotonic acid (Z-ct form)

		exp. (IR, Ar matrix)				calc. (6-31G*)			
approximate description	symmetry	ν	I	$\nu^{gc\,a}$	$I^{total\,b}$	ν	I	$\nu^{scaled\,c}$	PED[d]
ν(O—H)	A′	3557.7	7.0	3557.7	7.0	4054	9.8	3557	s_1[100]
ν(C_α—H)	A′	no				3391	0.6	3077	s_2[96]
ν(CH_3)$_{as}$	A′	no				3376	0.4	3064	s_4[83] + s_5[12]
ν(C_β—H)	A′	no				3327	1.4	3020	s_3[95]
ν(CH_3)$_{as}$	A″	2945.9	0.7	2945.9[e]	0.7	3245	2.1	2958	s_{21}[101]
ν(CH_3)$_s$	A′	no				3203	2.0	2908	s_5[87] + s_4[16]
ν(C=O)	A′	1746.7	17.8	1743.7	39.7	2016	47.9	1781	s_6[87]
		1741.2	21.9						
ν(C=C)	A′	no				1869	1.0	1654	s_7[75] + s_{12}[10]
δ(CH_3)$_{as}$	A″	no				1638	0.6	1447	s_{22}[91]
δ(CH_3)$_{as}$	A′	no				1626	0.3	1442	s_8[95]
δ(C_β—H)	A′	1413.8	3.1	1413.8	3.1	1579	2.4	1401	s_{12}[32] + s_9[22] + s_{11}[19] + s_{16}[11]
δ(CH_3)$_s$	A′	no				1565	2.5	1389	s_9[68]
ν(C—O) + δ(C—O—H)	A′	1338.8	4.1	1338.8	4.1	1504	4.9	1336	s_{10}[18] + s_{11}[31] + s_{13}[14] + s_{12}[13] + s_{17}[11]
δ(C_α—H)	A′	1263.3	1.2	1263.3	1.2	1403	1.1	1248	s_{11}[27] + s_{12}[24] + s_{13}[17]
δ(C—O—H) + ν(C—O)	A′	1223.0	1.8	1174.1	20.8	1345	16.8	1197	s_{13}[46] + s_{10}[28]
		1217.0	0.4						
		1168.5	18.6						
γ(CH_3) + γ(C_β—H)	A″	no				1202	<0.1	1063	s_{23}[44] + s_{25}[42]
γ(CH_3)	A′	1068.2	2.5	1068.2	2.5	1199	2.3	1070	s_{14}[50] + S_{20}[12] + s_{10}[12] + s_{11}[10]
γ(C_α—H)	A″	no				1123	0.3	993	s_{24}[47] + s_{23}[28] + s_{25}[14]
ν(C—C)	A′	no				1007	0.2	903	s_{15}[46] + s_{14}[19] + s_{16}[11]
ν(C_α—C)	A′	835.6	1.8	835.6	1.8	918	0.7	826	s_{16}[24] + s_{15}[23] + s_{10}[21] + s_{19}[12]
γ(C_β—H) + γ(CH_3)	A″	827.3	14.6	827.3	14.6	934	7.5	826	s_{25}[43] + s_{26}[22] + s_{23}[22]
δ(O=C—O)	A′	675.9	2.6	675.9	2.6	742	3.7	672	s_{17}[31] + s_{19}[41] + s_{20}[27] + s_{18}[12] + s_{14}[12] + s_{13}[10]
γ(C=O)	A″	661.5	1.9	661.5	1.9	744	0.7	658	s_{26}[45] + s_{23}[13] + s_{25}[13]
τC—O	A″	no				635	9.3	571	s_{27}[95]
δ(C—C=O)	A′	no				593	2.1	367	s_{18}[10] + s_{17}[50] + s_{16}[22]
δ(C—C_β=C)	A′	no				382	0.5	519	s_{20}[69] + s_{18}[58]
τ(C=C)	A″	no				359	0.1	320	s_{29}[75] + s_{26}[22]
δ(C=C_α—C)	A′	no				249	<0.1	233	s_{19}[54] + s_{18}[16]
τ(C—C)	A″	no				114	<0.1	111	s_{28}[95]
τ(C_α—C)	A″	no				47	0.1	54	s_{30}[106]

See Table 2 for all definitions except for non-normalized *ab initio* intensities (km mol^{-1}) which can be obtained by multiplying the values in the Table by 12.93.

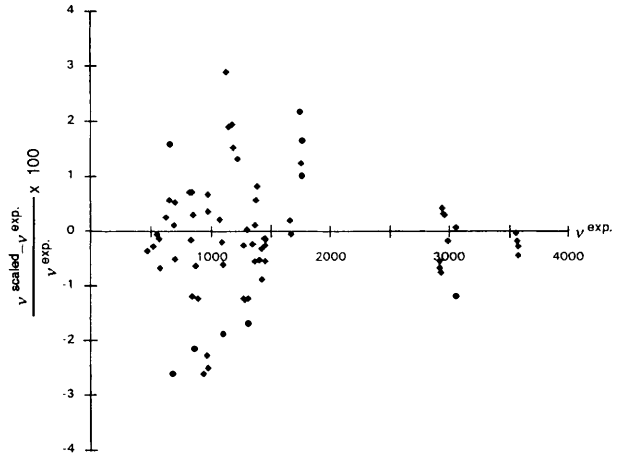

Fig. 10 Differences between the SCF-HF/6-31G* calculated (scaled) wavenumbers and the experimental values [100 ($\nu^{scaled} - \nu^{exp.}$)/$\nu^{exp.}$ %]. The scaled values were calculated from the optimized straight lines obtained by fitting calculated to experimental wavenumbers using two different linear regressions, one for in-plane vibrations, and the other for out-of-plane modes (see text). The straight lines obey the equations. ν^{scaled} (in-plane) = 0.870 × $\nu^{ab\ initio}$ + 25.8 (R^2 = 0.999 554); ν^{scaled} (out-of-plane) = 0.882 × $\nu^{ab\ initio}$ + 2.5 (R^2 = 0.999 445).

lated wavenumbers agree with the experimental values to within less than 1%.

In contrast to the ν(CH) vibrations, those modes involving the oxygen atoms give rise to the most intense IR bands, ν(C=O), δ(COH) + ν(C—O), and τ(C—O) dominating the spectra of both observed conformers of (*E*)-crotonic acid. Thus, the assignment of these bands could be made easily, being in consonance with the predicted intensity ratios (see Tables 2 and 3). It is very well known that some significant intensity variations occur in bands associated with vibrations of the carboxyl group in molecules as a consequence of internal rotation.[8] Thus, the good agreement found between experimental and calculated intensity ratios of the bands ascribed to the ν(C=O), δ(COH) + ν(C—O), and τ(C—O) vibrations in the two conformers [experimental *vs.* predicted $I_{E\text{-}ct}/I_{E\text{-}cc}$ are 1.5 *vs.* 1.8, 0.9 *vs.* 0.8 and 1.1 *vs.* 1.2 for, ν(C=O), δ(COH) + ν(C—O), and τ(C—O), respectively] strongly support the assignments made.

The normal coordinate analysis show that most of the vibrations are dominated by one internal symmetry coordinate (see Tables 2 and 3). However, as is usual for monomeric carboxylic acids,[9,15,29,31] ν(C—O) and δ(COH) are considerably mixed and thus, it appears to be more correct to consider, instead of 'pure' ν(C—O) and δ(COH) coordinates, 'hybrid' vibrations having significant contributions from

Table 6 Calculated vibrational wavenumbers (cm^{-1}) and intensities for the non-observed conformers of (*E*)-crotonic acid (E-tc and E-np)

		E-tc				E-np			
approximate description	symmetry[a]	ν	I	$\nu^{scaled\ b}$	PED[c]	ν	I	$\nu^{scaled\ b}$	PED[c]
ν(O—H)	A′	4121	4.6	3615	s_1[100]	4131	3.9	3624	s_1[100]
ν(C_β—H)	A′	3374	0.2	3062	s_3[99]	3324	2.0	3016	s_3[93]
ν(C_α—H)	A′	3336	1.0	3028	s_2[99]	3387	0.2	3074	s_2[99]
$\nu(CH_3)_{as}$	A′	3287	1.3	2984	s_4[98]	3292	0.6	2988	s_4[90]
$\nu(CH_3)_{as}$	A″	3257	1.3	2969	s_{21}[101]	3257	1.6	2970	s_{21}[101]
$\nu(CH_3)_s$	A′	3204	1.2	2909	s_5[98]	3204	1.6	2909	s_5[97]
ν(C═O)	A′	2040	20.1	1802	s_6[91]	2055	33.0	1815	s_6[91]
ν(C═C)	A′	1880	9.1	1663	s_7[72] + s_{12}[12] + s_{11}[10]	1884	1.2	1666	s_7[73] + s_{12}[13]
$\delta(CH_3)_{as}$	A′	1629	1.8	1445	s_8[92]	1630	0.7	1445	s_8[94]
$\delta(CH_3)_{as}$	A″	1622	0.4	1433	s_{22}[94]	1622	0.5	1433	s_{22}[95]
$\delta(CH_3)_s$	A′	1565	0.1	1389	s_9[104]	1568	0.6	1391	s_9[104]
ν(C—O) + δ(C—O—H)	A′	1502	18.7	1334	s_{10}[27] + s_{11}[35] + s_{16}[16] + s_{13}[11]	1585	31.8	1320	s_{10}[44] + s_{13}[31] + s_{16}[20] + s_{17}[14]
δ(C_α—H)	A′	1456	16.0	1294	s_{11}[17] + s_{12}[28] + s_{13}[21]	1425	0.5	1267	s_{11}[75]
δ(C_β—H)	A′	1422	6.3	1265	s_{12}[46] + s_{13}[25] + s_{11}[14]	1559	1.0	1297	s_{12}[70] + s_7[12]
δ(C—O—H) + ν(C—O)	A′	1284	1.1	1144	s_{13}[27] + s_{10}[29]	1319	1.8	1175	s_{13}[56] + s_{15}[12] + s_{16}[11]
$\gamma(CH_3)$	A′	1212	0.3	1081	s_{14}[29] + s_{15}[22] + s_{11}[15]	1207	0.2	1077	s_{14}[29] + s_{15}[36]
$\gamma(CH_3)$ + γ(C_β—H)	A″	1205	0.2	1065	s_{23}[43] + s_{25}[44]	1192	0.2	1054	s_{23}[54] + s_{25}[47]
γ(C_α—H)	A″	1094	2.1	968	s_{24}[58] + s_{23}[22] + s_{25}[19]	1115	2.9	986	s_{24}[69] + s_{25}[26] + s_{23}[11]
ν(C—C)	A′	1056	1.0	946	s_{15}[37] + s_{16}[25] + s_{10}[14]	1048	0.4	938	s_{15}[36] + s_{14}[21] + s_{10}[13] + s_{16}[11]
ν(C_α—C)	A′	984	0.2	883	s_{16}[24] + s_{14}[35] + s_{19}[12] + s_{15}[11] + s_{12}[10]	974	1.9	874	s_{16}[17] + s_{14}[18] + s_{24}[18] + s_{10}[16] + s_{26}[15]
γ(C_β—H) + $\gamma(CH_3)$	A″	939	2.3	831	s_{25}[37] + s_{23}[48]	939	1.6	830	s_{25}[43] + s_{23}[4]
γ(C═O)	A″	764	0.4	676	s_{26}[68] + s_{24}[20]	765	0.9	677	s_{26}[61] + s_{24}[12]
δ(O═C—O)	A′	741	0.8	671	s_{17}[60]	693	0.7	629	s_{17}[57] + s_{26}[16]
δ(C—C═O)	A′	516	0.3	475	s_{18}[53] + s_{17}[12] + s_{20}[12]	539	0.5	496	s_{18}[57] + s_{16}[11]
τ(C—O)	A″	470	8.3	417	s_{27}[96]	499	7.8	442	s_{27}[100]
δ(C—C_β═C)	A′	421	0.3	392	s_{20}[43] + s_{16}[15]	403	0.6	377	s_{20}[47] + s_{16}[12] + s_{27}[12] + s_{17}[11]
τ(C═C)	A″	215	0.2	192	s_{29}[92] + s_{26}[10]	196	0.3	176	s_{29}[94] + s_{19}[17] + s_{25}[13]
τ(C—C)	A″	210	0.2	188	s_{28}[83]	208	0.4	186	s_{28}[72] + s_{19}[17] + s_{30}[12]
δ(C═C_α—C)	A′	206	0.4	206	s_{19}[57] + s_{20}[28] + s_{26}[19]	227	0.2	223	s_{19}[27] + s_{28}[20] + s_{25}[15] + s_{20}[14]
τ(C_α—C)	A″	93	0.1	84	s_{30}[94]	104	0.4	94	s_{30}[84] + s_{28}[20]

Vibrations: ν, stretching; δ, bending; ω, wagging; γ, rocking; τ, torsion. no, not observed; s, symmetric; as asymmetric. See Table 8 for definition of coordinates. Calculated intensities are normalized to the total calculated intensity of all bands ($I = 100\ I^{calc}/\sum_{i=1,30} I_i^{calc}$). The non-normalized *ab initio* intensities (km mol^{-1}) can be obtained by multiplying the values presented in the Table by 17.09 and 15.29, respectively, for forms E-tc and E-np. [a] Local symmetry species; global symmetry species of all normal modes of the non-symmetric (C_1 point group) E-np conformer is A. [b] An additional correction factor (1.033) was applied specifically to the scaled C—H stretching wavenumbers resulting from the scaling; such an additional correction factor was obtained by linear regression constrained by assuming a zero intercept and performed using all observed/scaled ν(C—H) wavenumbers for all observed conformers. [c] PEDs < 10% are not presented in the Table.

Table 7 Calculated vibrational wavenumbers (cm^{-1}) and intensities for the non-observed conformer of (*Z*)-crotonic acid (*Z*-tc)

approximate description	symmetry	ν	I	$\nu^{scaled\ a}$	PED[b]
ν(O—H)	A′	4125	4.9	3618	s_1[100]
$\nu(CH_3)_{as}$	A′	3381	0.1	3068	s_4[84] + s_5[12]
$\nu(C_\alpha—H)$	A′	3344	1.7	3035	s_2[54] + s_3[43]
$\nu(C_\beta—H)$	A′	3319	0.7	3013	s_3[54] + s_2[46]
$\nu(CH_3)_{as}$	A″	3244	1.5	2958	s_{21}[101]
$\nu(CH_3)_s$	A′	3201	1.4	2907	s_5[88] + s_4[15]
ν(C=O)	A′	2038	18.5	1801	s_6[91]
ν(C=C)	A′	1867	8.3	1652	s_7[77]
$\delta(CH_3)_{as}$	A″	1641	0.6	1450	s_{22}[88]
$\delta(CH_3)_{as}$	A′	1624	3.3	1440	s_8[69] + s_{11}[14]
$\delta(C_\alpha—H)$	A′	1596	0.6	1416	s_{11}[29] + s_8[31] + s_{12}[23]
$\delta(CH_3)_s$	A′	1550	1.2	1375	s_9[92]
δ(C—O—H) + ν(C—O)	A′	1454	37.0	1291	s_{13}[55] + s_{10}[29 + s_{17}[10]
$\delta(C_\beta—H)$	A′	1410	1.3	1253	s_{12}[44] + s_{11}[19] + s_7[10]
ν(C—O) + δ(C—O—H)	A′	1282	1.4	1142	s_{10}[37] + s_{13}[27]
$\gamma(CH_3)$	A′	1216	0.7	1085	s_{14}[39] + s_{11}[13] + s_{20}[12] + s_{15}[11]
$\gamma(CH_3)$ + $\gamma(C_\beta—H)$	A″	1205	<0.1	1066	s_{23}[44] + s_{25}[43]
$\gamma(C_\alpha—H)$	A″	1100	0.1	972	s_{24}[45] + s_{23}[27] + s_{25}[23]
ν(C—C)	A′	1014	0.9	909	s_{15}[33] + s_{14}[26] + s_{16}[18]
$\nu(C_\alpha—C)$	A′	950	0.3	854	s_{16}[27] + s_{15}[35] + s_{19}[13]
$\gamma(C_\beta—H)$ + $\gamma(CH_3)$	A″	909	4.6	804	s_{25}[40] + s_{26}[27] + s_{23}[18] + s_{24}[11]
δ(O=C—O)	A′	784	1.1	708	s_{17}[35] + s_{19}[27] + s_{20}[17] + s_{18}[13] + s_{10}[11] + s_{14}[10]
γ(C=O)	A″	728	0.6	644	s_{26}[42] + s_{24}[31] + s_{23}[16] + s_{25}[12]
δ(C—C=O)	A′	571	0.1	523	s_{18}[24] + s_{17}[44] + s_{16}[20] + s_{20}[15]
τ(C—O)	A″	462	7.2	410	s_{27}[104]
$\delta(C—C_\beta=C)$	A′	401	0.2	375	s_{20}[60] + s_{18}[56]
τ(C=C)	A″	365	0.8	324	s_{29}[76] + s_{26}[22]
$\delta(C=C_\alpha—C)$	A′	245	0.6	239	s_{19}[54] + s_{18}[12]
τ(C—C)	A″	116	<0.1	105	s_{28}[104]
$\tau(C_\alpha—C)$	A″	23	0.2	23	s_{30}[96]

Vibrations: ν, stretching; δ, bending; ω, wagging; γ, rocking; τ, torsion. no, not observed; s, symmetric; as asymmetric. See Table 8 for definition of coordinates. Calculated intensities are normalized to the total calculated intensity of all bands ($I = 100\ I^{calc}/\sum_{i=1,30} I_i^{calc}$). The non-normalized *ab initio* intensities (km mol^{-1}) can be obtained by multiplying the values presented in the Table by 16.84. [a] An additional correction factor (1.033) was applied specifically to the scaled C—H stretching wavenumbers resulting from the scaling; such an additional correction factor was obtained by linear regression, constrained by assuming a zero intercept and performed using all observed/scaled ν(C—H) wavenumbers for all observed conformers. [b] PEDs < 10% are not presented in the Table.

these two coordinates [δ(COH) + ν(C—O) and ν(C—O) + δ(COH)]. Similar situations occur for $\gamma(CH_3)$ (a″) and $\gamma(C_\beta—H)$ in both the E-cc and E-ct conformers ['hybrid' coordinates, $\gamma(CH_3) + \gamma C_\beta—H$) and $\gamma(C_\beta—H) + \gamma(CH_3)$, are prefered] and for $\gamma(CH_3)$ (a′) and ν(C—C) in the E-ct form [in the E-cc conformer, the vibrational mixing involves the $\gamma(CH_3)$ (a′) and both the two ν(C—C) stretching modes: ν(C—C) and $\nu(C_\alpha—C)$, see Table 2]. For both conformers, the vibrations which can be approximately described as ν(C—O) + δ(COH), ν(C—C) and $\nu(C_\alpha—C)$ correspond to those modes where the mixing of coordinates is more extensive. It is important to note that such mixing makes these modes extremely sensitive to both conformation and chemical environment, thus making them suitable for use as IR spectroscopic probes for both conformer identification and characterization of the main intermolecular interactions involving this kind of molecule.

Finally, it is interesting to compare the calculated (or observed) ν(C=O) and ν(OH) frequencies of the two experimentally observed conformers with those predicted for the higher energy E-tc and E-np forms (Tables 2, 3 and 6). In fact, both these modes are predicted to occur at much higher frequencies in the latter conformers. These results can be correlated with the presence in the observed conformers of the previously mentioned C=O···OH through-space field interaction that increases the degree of polarization of both the C=O and OH bonds in these forms, leading to reduced force constants associated with the C=O and OH oscillators and, consequently, to lower ν(C=O) and ν(OH) vibrational frequencies. In addition, the predicted intensities of the ν(OH) IR bands of both the E-tc and E-np forms are considerably lower than in the two experimentally observed conformers. This result is in agreement with those previously obtained for acrylic acid[9] and, consequently, it can also be ascribed to a reduced charge-flux contribution to the ν(OH) IR band intensities in the non-observed conformers.

(Z)-Crotonic Acid The detailed analysis of the IR spectra of the two observed conformers of (*Z*)-crotonic acid (Z-cc and Z-ct; see Tables 4 and 5 and Fig. 9) indicates that at least the lower energy Z-cc form of this molecule is also trapped in two different sites [only one intense band doublet 1746.7/1741.2 cm^{-1} could be observed in the spectrum of the Z-ct form, and this may be a Fermi resonance doublet involving the ν(C=O) fundamental and the combination band ν(C—C) + $\nu(C_\alpha—C)$]. As in the case of (*E*)-crotonic acid, also for the Z-cc conformer of (*Z*)-crotonic acid the simultaneous occurrence of matrix site splitting and Fermi resonance gives rise to the appearance of bands presenting complex structure [*e.g.* ν(C=O), ν(C—O) + δ(C—O—H), $\gamma(C_\beta—H) + \gamma(CH_3)$, τ(C—O); see Table 4].

The following additional points shall be stressed:

(i) The calculated composition of normal coordinates in terms of internal coordinates for the various conformers of (*Z*)-crotonic acid points to a coordinate mixing similar to that found for (*E*)-crotonic acid. In particular, the [$\gamma(C_\beta—H)$; $\gamma(CH_3)$] and [ν(C—O); δ(C—O—H)] pairs of coordinates are best represented by their 'hybrid' coordinates. However, in the case of the Z-ct conformer, that coordinate best described as ν(C—O) + δ(C—O—H) appears at a higher frequency than that described as δ(C—O—H) + ν(C—O), in contrast to what succeeds for all other studied molecules (see Tables 2–7). Furthermore, in both observed conformers of (*Z*)-crotonic acid, the δ(O=C—O) coordinate corresponds to that having the highest degree of mixing, thus acquiring increased

Table 8 Definition of the internal symmetry coordinates used in the normal coordinate analysis

coordinate	approximate description	symmetry	definition
S_1	ν(O—H)	A′	ν(O—H)
S_2	$\nu(C_\alpha—H)$	A′	$\nu(C_\alpha—H)$
S_3	$\nu(C_\beta—H)$	A′	$\nu(C_\beta—H)$
S_4	$\nu(CH_3)_{as}$	A′	2ν[C—H(10)] − ν[C—H(11)] − ν[C—H(12)]
S_5	$\nu(CH_3)_s$	A′	ν[C—H(10)] + ν[C—H(11)] + ν[C—H(12)]
S_6	ν(C=O)	A′	ν(C=O)
S_7	ν(C=C)	A′	ν(C=C)
S_8	$\delta(CH_3)_{as}$	A′	2δ[H(11)—C—H(12)] − δ[H(10)—C—H(11)] − δ[H(10)—C—H(12)]
S_9	$\delta(CH_3)_s$	A′	δ[H(11)—C—H(12)] + δ[H(10)—C—H(11)] + δ[H(10)—C—H(12)] − δ[H(10)—C—C] − δ[H(11)—C—C] − δ[H(12)—C—C]
S_{10}	ν(C—O)	A′	ν(C—O)
S_{11}	$\delta(C_\alpha—H)$	A′	$\delta(H—C_\alpha=C) - \delta(H—C_\alpha—C)$
S_{12}	$\delta(C_\beta—H)$	A′	$\delta(H—C_\alpha—C) - \delta(H—C_\alpha=C)$
S_{13}	δ(C—O—H)	A′	δ(C—O—H)
S_{14}	$\gamma(CH_3)$	A′	2δ[H(10)—C—C] − δ[H(11)—C—C] − δ[H(12)—C—C]
S_{15}	ν(C—C)	A′	ν(C—C)
S_{16}	$\nu(C_\alpha—C)$	A′	$\nu(C_\alpha—C)$
S_{17}	δ(O=C—O)	A′	2δ(O=C—O) − δ(C—C=O) − δ(C—C—O)
S_{18}	δ(C—C=O)	A′	δ(C—C=O) − δ(C—C—O)
S_{19}	$\delta(C=C_\alpha—C)$	A′	$2\delta(C=C_\alpha—C) - \delta(H—C_\alpha=C) - \delta(H—C_\alpha—C)$
S_{20}	$\delta(C—C_\beta=C)$	A′	$2\delta(C—C_\beta=) - \delta(H—C_\beta—C) - \delta(H—C_\beta=C)$
S_{21}	$\nu(CH_3)_{as}$	A″	ν[C—H(11)] − ν[C—H(12)]
S_{22}	$\delta(CH_3)_{as}$	A″	δ[H(10)—C—H(11)] − δ[H(10)—C—H(12)]
S_{23}	$\gamma(CH_3)$	A″	δ[H(11)—C—C] − δ[H(12)—C—C]
S_{24}	$\gamma(C_\alpha—H)$	A″	γ[C=C_α(—H)—C]
S_{25}	$\gamma(C_\beta—H)$	A″	γ[C—C_β(—H)=C]
S_{26}	γ(C=O)	A″	γ[C—C(=O)—O]
S_{27}	τ(C—O)	A″	τ(H—O—C=O) + τ(H—O—C—C)
S_{28}	τ(C—C)	A″	τ[H(10)—C—C=C] + τ[H(11)—C—C=C] + τ[H(12)—C—C=C] + τ[H(10)—C—C—H] + τ[H(11)—C—C—H] + τ[H(12)—C—C—H]
S_{29}	τ(C=C)	A″	τ(H—C=C—C) + τ(C—C=C—C) + τ(H—C=C—H) + τ(C—C=C—H)
S_{30}	$\tau(C_\alpha—C)$	A″	τ(H—C—C=O) + τ(H—C—C—O) + τ(C=C—C=O) + τ(C=C—C—O)

Normalization constants are not given here; they are chosen as $N = (\sum c_i^2)^{-1/2}$, where c_i are the coefficients of the individual valence coordinates. Vibrations: ν, bond stretching; δ, in-plane bending, γ, rocking, τ, torsion. as, asymmetric; s, symmetric.

importance as an IR spectroscopic probe for the study of intermolecular interactions involving this molecule.

(ii) As compared with the corresponding modes in the two observed forms, both ν(C=O) and ν(OH) are predicted to occur at much higher frequencies in the non-observed Z-tc form. This is a similar trend to that observed in the case of (*E*)-crotonic acid and thus, can be ascribed to the same causes.

(iii) Finally, by comparing the relative frequencies of the corresponding vibrational modes of the (*Z*)- and (*E*)-crotonic acid conformers, the following bands can be selected as being those more suitable to distinguish between the two acids (*i.e.* those bands more sensitive to the position of the methyl substituent): $\delta(C_\beta—H)$ and δ(O=C—O), which are both blue shifted in *Z*-crotonic acid, and δ(COH) + ν(C—O), ν(C—C), $\nu(C_\alpha—C)$, $\gamma(C_\beta—H) + \gamma(CH_3)$ and γ(C=O), all being red shifted in this molecule. It is interesting to note that most of these modes predominantly involve coordinates that are directly affected by the change of position of the methyl group.

Photodecomposition of Crotonic Acid under UV Irradiation below 243 nm

As referred to before, upon UV irradiation at wavelengths smaller than 243 nm, crotonic acid begins to photodecompose. This can be easily detected spectroscopically, since characteristic bands of CO, CO_2 and H_2O appear in the spectrum of the sample after irradiation by non-filtered light [see Fig. 5(*a*)]. Very interestingly, the amount of CO_2 produced by the photodecomposition processes is considerably higher than that of both CO and H_2O.

In addition to the bands due to CO, H_2O and CO_2, other bands ascribable to crotonic acid photodecomposition products could be observed, which are attributed to formic acid, propene and a hydrogen-bonded complex of propyne with CO (Table 9). Since the adduct is a well isolated crotonic acid molecule, the photochemical transformations pertain to reactions confined to the matrix cage. This fact and stoichiometric considerations imply that CO is trapped together with H_2O and propyne, and CO_2 with propene. Most of the observed frequencies are slightly different from the literature values[35–40] (see Table 9), clearly indicating that the products of photodecomposition which are trapped in the same matrix cage are interacting with each other. In particular, the frequencies of CO were measured at 2147.4, 2138.2 and 2130.1 cm^{-1}, the highest frequency band corresponding to a frequency typical of a hydrogen-bonded complex of CO.[38–40] Thus, the results indicate that under irradiation below 243 nm, crotonic acid decomposes following two main pathways:

$$\text{(I)}\quad CH_3—CH=CH—COOH \rightarrow CH_3—CH=CH_2 + CO_2$$

$$\text{(II)}\quad CH_3—CH=CH—COOH \rightarrow CH_3—C\equiv CH + CO + H_2O$$

with the primary photoproducts of (II) acting as reactants in one of the two secondary processes (IIa) or (IIb):

$$\text{(IIa)}\quad CH_3—C\equiv CH + CO \rightarrow CH_3—C\equiv CH\cdots CO$$

$$\text{(IIb)}\quad CO + H_2O \rightarrow HCOOH$$

Since among the bands originating from the photodecomposition products, those ascribed to CO_2 and formic

Table 9 Observed IR wavenumbers (cm^{-1}), relative intensities and vibrational assignments for the products of photodissociation of crotonic acid

assignment	molecule[a]	symmetry	ν^b	I^c	$\nu^{gc\ d}$	$\nu^{lit\ e}$
ν(O—H)	FA	A′	3571.5	S	3571.5	3570
ν(CH)	P	A′	3043.1	vw	3043.1	*3017*
$\nu(CH_2)$	P	A′	3004.1	vw	3004.1	2991
ν(C—H)	FA	A′	2910.1	vw	2910.1	2938
ν(C≡C)	Pry–CO	A_1	1980.3	vw	1967.5[f]	
			1978.1	vw		
			1944.2	vw		
ν(C=O)	FA	A′	1775.7	vS	1775.7	1774
$\delta(CH_3)_{as}$	P	A″	1429.5	w	1429.5	1442
$\delta(CH_2)$	P	A′	1408.3	w	1408.3	*1419*
δ(CH)	FA	A′	1373.2	w	1369.4	1380
			1368.2	m		
$\delta(C—H)_{ip}$	P	A′	1289.3	w	1289.3	1298
$\omega(CH_2)$	P	A′	1191.6	vw	1191.6	1174
ν(C—O)	FA	A′	1111.0	m	1107.0	1103
			1107.4	S		
			1104.9	S		
$tw(CH_2)$	P	A″	995.4	m	995.4	990
$\gamma(CH_3)$	P	A′	936.0	w	935.5	*945*
			935.0	w		
$\gamma(CH_2)$	P	A″	928.6	w	919.7	912
			917.0	S		
ν(C—C)	P	A′	872.6	vw	853.8	*840*
			844.5	w		
τ(C—O)	FA	A″	655.7	w	639.0	638
			634.0	S		
δ(O=C—O)	FA	A′	622.9	m	622.9	626
$\delta(C—H)_{oop}$	P	A″	558.6	w	558.6	575
δ(C—H)	Pry–CO	E	548.7	w	519.5	
			503.8	w		
δ(C—C=C)	P	A′	454.2	w	454.2	428

Vibrations: ν, stretching; δ, bending; ω, wagging; γ, rocking; τ, torsion; s, symmetric; as asymmetric; ip, in-plane; oop, out-of-plane. Bands due to CO, CO_2 and H_2O not shown. [a] FA, Formic acid; P, Propene; Pry–CO, hydrogen-bonded complex involving CO and propyne. [b] An additional doublet of bands with components at 778.1 (w) and 753.6 (vw) cm^{-1} (gravity centre: 768.9 cm^{-1}) also appears in the spectrum; although its assignment cannot be unambiguously made, it is possible that the bands correspond to the δ(CH) π_u mode of acetylene.[35] [c] vS, very strong; S, strong; m, medium; w, weak; vw, very weak. [d] ν^{gc} correspond to the wavenumber of the gravity centres of the groups of bands ascribed to the same normal mode; they are calculated from $\nu^{gc} = \sum_i(\nu^{obs}I^{obs})/\sum_i I^{obs}$, where i is the number of total components of the group of bands. [e] ν^{lit} correspond to wavenumbers taken from literature. Data for FA and P were taken from ref. 36 and 37, respectively (values in italic were calculated[36,37]). The two bands ascribed to the complex involving propyne have counterparts in the free molecule at 2142 cm^{-1} [ν(C≡C)] and 633 cm^{-1} [δ(CH)].[35] [f] Gravity-centre wavenumber calculated assuming equal intensities for the three observed components which have an intensity too low to enable a quantitative measurement of their relative intensity.

acid are the most intense, the favoured reactions appear to be (I) and (II) → (IIb). Note that the prevalence of (IIb) over (IIa) justifies, at least in part, the considerably lower amount of CO detected spectroscopically.

We are currently studying the photodecomposition of acrylic acid in matrices, including the product yield dependence on precursor conformation, and these studies may also shed light on the influence of conformation on the photodecomposition processes of crotonic acids under similar conditions.

This research was made possible in part by Grant N° R28300 from the International Science Foundation and the Russian Government. R.F. acknowledges the financial support from Junta Nacional de Investigação Científica e Tecnológica, J.N.I.C.T., Lisboa.

References

1 V. Vijayakakshmi, J. N. R. Vani and N. Krishnamurti, *Eur. Polym. Paint Colour J.*, 1991, **181**, 506.
2 K. Katada, H. Sano, Y. Katoh, V. K. Jain, S. Mashita, A. Takenchi and S. Koga, *Acta Radiol. Suppl.*, 1986, **369**, 623.
3 A. N. Brito, N. Correia, S. Svensson and H. Ågren, *J. Chem. Phys.*, 1991, **95**, 2965.
4 P. R. Carey, *Biochemical Applications of Raman and Resonance Raman Spectroscopies*, Academic Press, London, 1982.
5 P. J. Tonge and P. R. Carey, *Biochemistry*, 1990, **29**, 10723.
6 R. Fausto, *Ciên. Biol.*, 1988, **13**, 1.
7 K. Fan and J. E. Boggs, *J. Mol. Struct.*, 1987, **157**, 31.
8 S. W. Charles, F. C. Cullen, N. L. Owen and G. A. Williams, *J. Mol. Struct.*, 1987, **157**, 17.
9 A. Kulbida, M. N. Ramos, M. Rasanen, J. Nieminen, O. Schrems and R. Fausto, *J. Chem. Soc., Faraday Trans.*, 1995, **91**, 1571.
10 P. J. Tonge, M. Pusztai, A. J. White, C. W. Wharton and P. R. Carey, *Biochemistry*, 1991, **29**, 4790.
11 Y. Shindo, K. Horie and I. Mita, *J. Photochem.*, 1984, **26**, 185.
12 B. L. Stoddard, J. Bruhnke, N. Porter, D. Ringe and G. A. Petsko, *Biochemistry*, 1990, **29**, 4871.
13 J. R. Cowles, W. O. George and W. G. Fateley, *J. Chem. Soc., Perkin Trans. 2*, 1975, 396.
14 M. D. G. Faria, J. J. C. Teixeira-Dias and R. Fausto, *Vib. Spectrosc.*, 199, **2**, 107.
15 M. D. G. Faria, *Análise Conformacional e Vibracional de Compostos Carbonílicos α,β-Insaturados e Suas Interacções com Fenóis*, Departamento de Química, Universidade de Coimbra, Portugal, Internal Report, 1989.
16 W. R. Feairheller Jr. and J. E. Katon, *Spectrochim. Acta, Part A*. 1967, **23**, 2225.
17 K. B. Wiedberg and K. E. Laidig, *J. Am. Chem. Soc.*, 1987, **109**, 5935.
18 S. E. Galembeck and R. Fausto, *J. Mol. Struct. (Theochem.)*, 1995, **332**, 105.

19 A. Kulbida and A. Nosov, *J. Mol. Struct.*, 1992, **265**, 17.
20 W. J. Hehre, R. Ditchefield and J. A. Pople, *J. Chem. Phys.*, 1972, **56**, 2257.
21 M. J. Frisch, G. W. Trucks, M. Head-Gordon, P. M. W. Gill, M. W. Wong, J. B. Foresman, B. J. Johnson, H. B. Schlegel, M. A. Robb, E. S. Replogle, R. Gomperts, J. L. Andres, K. Raghavachari, J. S. Binkley, C. Gonzalez, R. L. Martin, D. J. Fox, D. J. Defrees, J. Baker, J. J. P. Stewart and J. A. Pople, *GAUSSIAN 92 (Revision C)*, Gaussian Inc., Pittsburgh PA, 1992.
22 H. B. Schlegel, Ph.D. Thesis, Queen's University, Kingston, Ontario, Canada, 1975.
23 M. D. G. Faria and R. Fausto, *TRANSFORMER (version 1.0)*, Departamento de Química, Universidade de Coimbra, Portugal, 1990.
24 M. D. G. Faria and R. Fausto, *BUILD-G and VIBRAT*, Departamento de Química, Universidade de Coimbra, Portugal, 1990 (These programs incorporate several routines from programs GMAT and FPERT, H. Fuher, V. B. Kartha, K. G. Kidd, P. J. Krueger and H. H. Mantsch, *Natl. Res. Council Can. Bull.*, 1976, **15**, 1).
25 M. D. G. Faria, J. J. C. Teixeira-Dias and R. Fausto, *Vibrat. Spectrosc.*, 1991, **2**, 43.
26 P. Carmona and J. Moreno, *J. Mol. Struct.*, 1982, **82**, 177.
27 J. J. C. Teixeira-Dias and R. Fausto, *J. Mol. Struct.*, 1986, **144**, 199.
28 R. Fausto and J. J. C. Teixeira-Dias, *J. Mol. Struct.*, 1986, **144**, 215; 225; 241.
29 A. Kulbida and R. Fausto, *J. Chem. Soc., Faraday Trans.*, 1993, **89**, 4257.
30 R. Fausto and J. J. C. Teixeira-Dias, *J. Mol. Struct. (Theochem.)*, 1987, **150**, 381.
31 R. Fausto, F. P. S. C. Gil and J. J. C. Teixeira-Dias, *J. Chem. Soc., Faraday Trans.*, 1993, **89**, 3235.
32 A. J. Barnes, in *Matrix Isolation Spectroscopy*, ed. A. J. Barnes, W. J. Orville-Thomas, A. Muller and R. Gaufres, D. Reidel, Dordrecht, 1981, p. 531.
33 K. Bolton, D. G. Lister and J. Sheridan, *J. Chem. Soc., Faraday Trans. 2*, 1974, **70**, 113.
34 R. Fausto, *J. Mol. Struct.*, submitted.
35 T. Shimanouchi, *Tables of Molecular Vibrational Frequencies*, National Standard Reference Data Series, National Bureau of Standards, Washington, DC, 1972.
36 H. Hollenstein and Hs. H. Gunthard, *J. Mol. Spectrosc.*, 1980, **84**, 457.
37 B. Silvi, P. Labarbe and J. P. Perchard, *Spectrochim. Acta, Part A*, 1973, **29**, 263.
38 H. Dubost and L. Abouaf-Marguin, *Chem. Phys. Lett.*, 1972, **17**, 269.
39 H. Dubost, *Chem. Phys.*, 1976, **12**, 139.
40 R. P. Muller, H. Hollenstein and J. R. Huber, *J. Mol. Spectrosc.*, 1983, **100**, 95.

Paper 5/03542B; *Received* 2nd *June*, 1995